T.C.
ANTALYA BILIM UNIVERSITY
INSTITUTE OF POSTGRADUATE EDUCATION
ELECTRICAL AND COMPUTER ENGINEERING
(THESIS - ENGLISH)

NOVEL WAVEFORM DESIGNS FOR FUTURE WIRELESS SYSTEMS: NON-COHERENT ORTHOGONAL FREQUENCY DIVISION MULTIPLEXING WITH SUBCARRIER POWER MODULATION (NC-OFDM-SPM) & MULTI-USER AUXILIARY SIGNAL SUPERPOSITION TRANSMISSION (MU-AS-ST)

DISSERTATION

PREPARED BY
MOHAMEDOU ABEWA

ANTALYA - 2021

T.C.
ANTALYA BILIM UNIVERSITY
INSTITUTE OF POSTGRADUATE EDUCATION
ELECTRICAL AND COMPUTER ENGINEERING
(THESIS - ENGLISH)

NOVEL WAVEFORM DESIGNS FOR FUTURE WIRELESS SYSTEMS: NON-COHERENT ORTHOGONAL FREQUENCY DIVISION MULTIPLEXING WITH SUBCARRIER POWER MODULATION (NC-OFDM-SPM) & MULTI-USER AUXILIARY SIGNAL SUPERPOSITION TRANSMISSION (MU-AS-ST)

DISSERTATION

PREPARED BY
MOHAMEDOU ABEWA

Dissertation/Project Advisor
Asst. Prof. Dr. JEHAD M. HAMAMREH

ANTALYA - 2021

APPROVAL/NOTIFICATION FORM
ANTALYA BİLİM UNIVERSİTY
INSTITUTE OF POST-GRADUATE EDUCATION

Mohamedou ABEWA, a master student of Antalya Bilim University, Institute of Post Graduate Education, Electrical and Computer Engineering with student ID 191212015, successfully defended the thesis/dissertation entitled "Novel waveform designs for future wireless systems: Non-Coherent OFDM with Subcarrier Power Modulation (NC-OFDM-SPM) & Multi-User Auxiliary Signal Superposition Transmission (MU-ASST)", which he prepared after fulfilling the requirements specified in the associated legislations, before the jury whose signatures are below.

	Academic Title / Name, Surname	**Signature**
Jury Member (Chairman):	Asst. Prof. Dr. Jehad HAMAMREH	.....
Jury Member:	Asst. Prof. Dr. Deniz GENÇAĞA	.....
Jury Member:	Asst. Prof. Dr. Ahmet YAZAR	.....
Director of The Institute:	Prof. Dr. İbrahim Sani MERT	.....

Thesis Submission Date: 01 / 06 / 2021

Thesis Defence Exam Date: 10 / 06 / 2021

I hereby declare that all information in this document has been obtained and presented in accordance with academic rules and ethical conduct. I also declare that, as required by these rules and conduct, I have fully cited and referenced all material and results that are not original to this work.

20 / 05 / 2021

Mohamedou ABEWA

ACKNOWLEDGEMENT

During this research journey, i would like to express my gratitude to many amazing people who made this journey unique for me.

First, i would like to express my deepest gratitude and thanks to my advisor during this work *Dr. Jehad HAMAMREH* for his extensive help, continuous guidance and motivation. Thank you for offering an amazing work environment for me during all this process. It was a great experience being a researcher in your wireless laboratory WISLAB.

I am so thankful to the jury members *Dr. Deniz GENÇAĞA* and *Dr. Ahmet YAZAR* for being part of this thesis. Your comments are crucial for the confirmation of the ideas developed in this manuscript and their correction in the presence of any gaps. Thank you so much.

I would like to dedicate this effort to my dear friends *Abdulwahab HAJAR* and *Youcef BELALLOU* who started the OFDM-SPM project with me as an undergraduate final year project. You are awesome.
This is also dedicated to *Lemayian Joel PONCHA* for his fruitful collaboration during this project. It was nice to work with you friend. With the wish of working on more exciting projects in the future.

Outside the thesis field of research, I would like to dedicate this work to the following list of amazing people for their collaboration, support and inspiration:

- *Dr. Sevgi ŞENGÜL*. Hocam, Thank you so much for the time i spent in your mathematical modelling project. I dedicate this thesis to you. You inspired me and helped me so much. I gained so much experience from your project which made this journey much easier for me. It was nice to meet you on the way. Thank you.
- *Dr. Deniz GENÇAĞA, Dr. Hakan ŞİMŞEK, Dr. Semail ÜLGEN*. Thank you very much professors for including me, at some point, in your research works. I would like to express my deepest thanks to you. I am indebted to all of you for sharing some of your experience with me.
- *Ahmet Kürşad SIRCAN*. This thesis is dedicated to you my amazing friend. Thanks for your amazing collaboration on the biophysics/modelling project, you taught me so much during this project. Thanks for the coffee talks on research and life. Thanks for your family too.
- *Mehmet OĞULCAN, Nestor ALAGUNA, Yacine MAROUF*. Thank you. This is also dedicated to you. Thank you for the discussions on wireless and other things.
- *Mohamed SALECK, Abderrahmane TALEB EBEIDY, Mohamed ELJIYID, Issa N'TAGHRY*. This is also dedicated to you guys. Thank you so much for your help during this period. It was great to keep contact with you all.

- *Abdou Ahmed SALEM and the Mauritanian Friends in Antalya.* Thank you so much for the nice time we had together in this period. Nice to meet you all.
- *Housemates and Antalya Friends.* Thank you Tareq, Cerullo, Yelzhas, Ibrahim, Ihab and the rest. This effort is dedicated to you. It was a privilege to meet all of you during this period.
- *Haris & Umair.* Thank you for the time we shared together, friends. Thank you for including me in the finance project in this period. Wishing fruitful collaborations for us in the future.
- I would like to dedicate this work to an amazing university worker Mehmet USTA with whom i spent good times. RIP. Thank you for the tea discussions on poetry, music and life. You were an amazing soul. May your soul be blessed.
- *Family.* Last, but not least this is dedicated to my amazing family members for their always unconditional and continuous support.
  This is particularly dedicated to my amazing girl friend. Thanks for your presence, Love.

Beautiful People,

Thank you so much.
Çok teşekkür ederim.

شكرا جزيلا.

Merci Beaucoup.
Muchas gracias.

Mohamedou ABEWA

ÖZET

GELECEKTEKİ KABLOSUZ SİSTEMLER İÇİN YENİ DALGA ŞEKLİ TASARIMLARI: EŞEVRELİ OLMAYAN OFDM İLE ALT TAŞIYICI GÜÇ MODÜLASYONU (NC-OFDM-SPM) & ÇOK KULLANICI YARDIMCI SİNYAL SÜPERPOZİSYON İLETİMİ (MU-ASST)

Gelecekteki kablosuz sistemlerin, spektral verimliliği ve iletim güvenilirliğini artırmak,iletimi güvence altına almak ve düşük karmaşıklık ve düşük gecikmeli iletişimleri garanti etmek gibi çok zorlu gereksinimleri karşılaması beklenmektedir. Bu kapsamda, bu çalışma içerisinde gelecekteki kablosuz sistemler için etkili bir tasarım sağlamak için bazı umut verici araştırma yönlerini araştırıyor ve öneriyoruz: 1) spektral verimliliği artırmak ve gelecekteki kablosuz sistemlerin tasarımındaki karmaşıklığı azaltmak için çok boyutlu OFDM modülasyonları ve eşevreli olmayan (non-coherent) modülasyon tabanlı tekniklerin kombinasyonunu inceliyoruz. Özellikle,bu bağlamda, alıcı kullanıcı / cihaz başına spektral verimliliği iki katına çıkarmak için Non-Coherent Orthogonal Frequency Division Multiplexing with Subcarrier Power Modulation(NC-OFDM-SPM) olarak adlandırılan yeni bir teknik öneriyor ve üzerinde çalışıyoruz. Ek bitler, bir OFDM bloğu içindeki alt taşıyıcıların gücünün ek bilgi iletimi için ek bir boyut olarak manipülasyonu yoluyla gönderilir. Ayrıca eşevreli olmayan (non-coherent) modülasyonun kullanılması, bu teknikte düşük tasarım karmaşıklığı sağlamaktadır. 2) Gelecekteki etkili ve güvenli çoklu erişim iletişimleri için yeni bir fiziksel katman güvenliği tasarımı öneriyoruz. Önerilen tasarım, Multi-User Auxiliary Signal Superposition Transmission (MU-AS-ST) olarak adlandırılır ve mevcut geleneksel Power Domain NOMA için alternatif bir tasarım olarak sunulur. Power Domain NOMA, sürüm 17'deki çalışma öğelerinden çıkarılmadan önce, sürüm 13'ten 16'ya kadar 3GGP (3. Nesil Ortaklık Projesi/ 3rd Generation Partnership Project) tarafından Multi-User Superposition Transmission (MUST) adı altında incelenmiştir. Önerilen tasarım, kullanıcı verilerinin üzerine bindirilmiş yardımcı sinyalleri kullanarak hem dahili (güvenilmeyen meşru kullanıcı) hem de harici dinleyicilere karşı mükemmel gizlilik sağlarken, kullanıcılar arası müdahaleyi (inter-user interference) tamamen iptal etmektedir. MU-AS-ST, geleneksel NOMA'dan daha iyi güvenilirlik sağlar ve Successive Interference Cancellation (SIC) kullanmamaktadır. Dahası, bu tasarım, yalnızca eşleştirilmiş (veya süper empoze edilmiş) kullanıcılar arasında önemli bir kanal farkının olduğu durumlarda çalışan geleneksel NOMA'nın aksine, baz istasyonuna olan uzaklıklarından bağımsız olarak herhangi iki kullanıcının kombinasyonu için çalışır. Ayrıca, tüm işlemlerin baz istasyonuna taşınması, bu tasarımı IoT cihazları gibi işlemle sınırlı iletişim cihazları için cazip bir seçim haline gelir. 3) Kablosuz iletişim için ayrılan spektrumun daha optimum kullanımı için alan ve cihaz başına spektral verimliliği artırmak için çoklu erişim kurulumlarında çok boyutlu OFDM modülasyon formatlarının entegrasyonunu inceliyoruz. Bu çalışmada, OFDM-SPM'nin MU-AS-ST ile kombinasyonunu inceliyoruz, burada bu kombinasyonun alan ve cihaz başına spektral verimliliği iki katına çıkardığını gösteriyoruz. Önerilen tasarımlar, spektral verimlilik, iletim güvenilirliği, tasarım karmaşıklığı ve tepe / ortalama güç oranı (PAPR) gibi farklı performans ölçütleri açısından kapsamlı bir şekilde incelenmiştir.

Anahtar Kelimeler: alt taşıyıcı güç modülasyonu, düşük karmaşıklık, eşevreli olmayan (non-coherent) modülasyon, fiziksel katman güvenliği, gizli dinleme, güvenilirlik, güç alanı NOMA, IoT, kablosuz iletişim, spektral verimlilik, yardımcı sinyaller, çok boyutlu OFDM, çoklu erişim.

ABSTRACT

NOVEL WAVEFORM DESIGNS FOR FUTURE WIRELESS SYSTEMS: NON-COHERENT OFDM WITH SUBCARRIER POWER MODULATION (NC-OFDM-SPM) & MULTI-USER AUXILIARY SIGNAL SUPERPOSITION TRANSMISSION (MU-ASST)

Future wireless systems are expected to serve very challenging requirements such as enhancing the spectral efficiency and transmission reliability, securing the transmission and guaranteeing low-complexity and low latency communications. In this scope, we investigate and propose in this work some promising research directions for ensuring an effective design for future wireless systems: 1) we study the combination of multi-dimensional OFDM modulations and non-coherent detection for enhancing the spectral efficiency and reducing the complexity in the design of future wireless systems. Particularly, in this regard, we propose and study a new technique termed as 'Non-Coherent Orthogonal Frequency Division Multiplexing with Subcarrier Power Modulation (NC-OFDM-SPM)' for doubling the spectral efficiency per receiving user/device through the exploration of the power of the subcarriers inside an OFDM block as an additional dimension for conveying extra information. The use of non-coherent detection ensures low-design complexity in this idea. 2) We propose a novel physical layer security design for effective and secure future multiple access communications. The proposed design is called 'Multi-User Auxiliary Signal Superposition Transmission (MU-AS-ST)' which is presented as an alternative design for the current conventional Power Domain NOMA which was studied by the 3GGP (3rd Generation Partnership Project) from release 13 till 16 under the name 'Multi-User Superposition Transmission (MUST)' before being eliminated from the study items in release 17. The proposed design superimposes auxiliary signals with the users data for cancelling the inter-user interference fully while achieving perfect secrecy against both internal (presence of an untrusted legitimate user) and external eavesdroppers. MU-AS-ST achieves better reliability than conventional NOMA and does not use Successive Interference Cancellation. Moreover, this design works for the combination of any two users regardless of their distance from the base station unlike conventional NOMA which works only for the cases where there exists a significant path-loss channel difference between paired (or super-imposed) users. Furthermore, carrying all the processing at the base station makes this design an appealing choice for processing-restricted communication devices such as IoT devices. 3) We study the integration of multi-dimensional OFDM modulation formats in multiple access setups for enhancing the spectral efficiency per area and per device for a more optimal usage of the spectrum allocated for wireless communications. As an example of this integration, we study the combination of OFDM-SPM with MU-AS-ST where we show that this leads to doubling the spectral efficiency per area and per device. The proposed designs were studied thoroughly and their performance was evaluated in terms of different performance metrics such as bit error rate, spectral efficiency, design complexity and peak to average power ratio (PAPR).
Keywords: auxiliary signals, eavesdropping, IoT, low-complexity, multi-dimensional OFDM, multiple access, non-coherent detection, physical layer security, power domain NOMA, reliability, spectral efficiency, subcarrier power modulation, wireless communications.

Contents

List of Tables

List of Figures

ABBREVIATIONS

3GPP 3rd Generation Partnership Project

AR Augmented Reality

AWGN Additive White Gaussian Noise

B5G Beyond 5G

BER Bit Error Rate

FDM Frequency Division Multiplexing

IBFD In-Band Full Duplex

IoT Internet of Things

MIMO Multiple-Input and Multiple-Output

MU-AS-ST Multi-User Auxiliary Signal Superposition Transmission

MU-LP Multi-User Linear Precoding

MU-MIMO Multi-User MIMO

MUST Multi-User Superposition Transmission

NOMA Non Orthogonal Multiple Access

OFDM Orthogonal Frequency Division Multiplexing

OFDM-IM OFDM with Index Modulation

OFDM-PSM OFDM Pulse Superposition Modulation

OFDM-SGM OFDM with Subcarrier Gap Modulation

OFDM-SNM OFDM with Subcarrier Number Modulation

OFDM-SPM OFDM with Subcarrier Power Modulation

OMA Orthogonal Multiple Access

PD-NOMA Power Domain Non Orthogonal Multiple Access

PLS Physical Layer Security

PN Phase Noise

PSK Phase Shift Keying

QAM Quadrature Amplitude Modulation

SIM-OFDM Subcarrier Index Modulation OFDM

SIM-OFDM Spatial Modulation OFDM

URLLC Ultra-Reliable Low Latency Communications

V2X Vehicle-to-Everything

eMBB Enhanced Mobile Broadband

mMTC massive Machine-Type Communications

mm-Wave millimeter Wave

self-het OFDM self-heterodyne OFDM

Notation

Vector and matrix notations are given in Table 1.

Table 1: Notation

	Time domain	Frequency domain
Vectors	x	$\boldsymbol{x}$
Matrices	H	$\boldsymbol{H}$

Chapter 1

Introduction

1.1 Motivation

Approximately, in every decade a new generation of wireless systems is being developed to address a set of communication requirements of that decade. Particularly, this era is characterized with the rise of the internet of things (IoT) where billions of devices which are equipped with sensing, communication and control capabilities are being interconnected. Moreover, with the massive spread in mobile devices and the emergence of new applications (e.g., extended reality, haptics, mission critical applications, ...etc), future networks (i.e., B5G/6G) should introduce novel transmission designs which are able to cope with this reality.
In the following, we discuss some important communication requirements in the light of the present and future wireless communication developments.

- *Spectral efficiency (i.e., Capacity)*: This requirement is very crucial in the current era. For serving a massive interconnection of data-hungry devices, we are in front of a very challenging task due to the scarcity of the spectrum allocated for wireless communications; the so called the spectrum shortage problem. Possible solutions to this problem is by licensing new part of the spectrum (i.e., millimeter wave / mm-wave) or developing novel transmission designs which are very efficient in using the available amount of licensed wireless spectrum. (i.e., doing more with less).

- *Wireless Security*: Due to the broadcast nature of electromagnetic signals used in wireless communications, the transmitted signals are prone to eavesdropping / hacking activities. As such, securing the data embedded in these signals is a must. This is further gaining importance in this era of digitalization where the scope of sensitive information is expanding including sensitive messages, phone/video calls, financial transactions, sharing secure documents … etc. Securing these data is a very crucial requirement which must be addressed by future wireless systems.

- *Transmission Reliability*: This is particularly important in sensitive application scenarios where ultra-reliability is a main requirement such as in the case of autonomous driving / vehicle-to-everything (V2X), remote diagnosis and surgery / augmented reality (AR)-assisted surgery, ..etc.

- *Complexity & Latency*: This is an era of speed and as such future systems are expected to take this aspect into account by developing techniques of low-latency characteristics. Another crucial concern which is significantly linked with latency is the design complexity where reducing the complexity of the design ensures lower latency timing.
  Developing schemes with low-complexity and low-latency is particularly important in the case of processing-restricted devices which are limited by their battery life.

- *Power Consumption*: It is very crucial that the developed techniques take into account the requirement of low power consumption especially if the developed designs are for low-power applications such as IoT applications.

The design challenges and requirements mentioned above, motivate and drive the development of novel transmission techniques for meeting the demands of future wireless systems.

1.2 Scope & Contributions

In this scope, this work proposes new designs for addressing the challenging requirements of future wireless systems by exploring many powerful and promising research directions such as the use of non-coherent designs for reducing the complexity and the latency of the communication, the use of multi-dimensional Orthogonal Frequency Division Multiplexing (OFDM) modulation formats and multiple access inspired designs for enhancing the spectral efficiency and reliability, and the use of Physical Layer Security (PLS) for a secure wireless data transmission.
This thesis proposes three novel techniques for future wireless communication systems. The main ideas involved in the design of the proposed techniques can be summarized as follows:

1. *Design 1 / NC-OFDM-SPM*: Non-Coherent OFDM with Subcarrier Power Modulation (NC-OFDM-SPM) is proposed as a novel non-coherent OFDM modulation technique where the power of the subcarriers inside an OFDM block is explored as an additional dimension for carrying extra information. This results in a technique featured with low-complexity due to the use of non-coherent detection, doubling the spectral efficiency per device compared to conventional OFDM where data is conveyed only through the classical constellation symbols (PSK or QAM), and the flexibility regarding the use of the transmit power where different power scenarios are formulated including power saving policy where, compared to conventional OFDM formats, some of the power can be saved to match the requirements of low power applications and the power reassignment policy where the saved power is reassigned to the transmit subcarriers to enhance the transmission reliability.

2. *Design 2 / MU-AS-ST*: This design proposes a novel and secure multiple access alternative for power domain NOMA. The proposed design makes use of auxiliary signal superposition where channel-dependent auxiliary signals are added

on top of the multiplexed users' signals, which are transmitted from different antenna sources in such a way that the transmission is secure against both external and internal (legitimate untrusted users) eavesdroppers. Moreover, it achieves a very good transmission reliability and low-complexity at the receiver by carrying all the complex processing tasks at the base station.

3. *Design 3 / D-SEAD*: Doubling the Spectral Efficiency per Area and per Device (D-SEAD) is a new technique proposed for a more efficient and secure usage of the wireless spectrum allocated for wireless systems. This design proposes the integration of multi-dimensional OFDM modulation formats in multiple access setups as a means of enhancing the spectral efficiency per area and per device. In particular, MU-AS-ST (i.e., Design 2) was modulated through a technique called OFDM with Subcarrier Power Modulation and Binary Phase Shift Keying (OFDM-SPM-BPSK) as an example of this general integration. Note that this modulation scheme is the coherent version of NC-OFDM-SPM. The integration of this modulation format in a multiple access setup yields doubling the spectral efficiency per area and per receiving device/user.

The capability of the proposed designs in addressing the challenges and requirements of future systems was studied through extensive computer simulations and mathematical derivations. The developed system models are explained in detail and are compared to state-of-the-art techniques in the literature.

Chapter 2

Non-Coherent OFDM with Subcarrier Power Modulation (NC-OFDM-SPM)

2.1 Introduction

For addressing the challenging requirements of future wireless systems, researchers have proposed and designed different techniques with varying levels of success. Among these developments, two particular research directions have gained importance in the wireless literature showing their promising potential in addressing the very challenging design requirements of future wireless communication systems.

2.1.1 Direction 1 / Multi-dimensional OFDM Modulations

One of the crucial requirements that are imposed on wireless systems and needs to be addressed urgently is the spectral efficiency requirement. In this regard, different techniques have been proposed in the literature for increasing the spectral efficiency of future wireless systems. The proposed schemes can be classified into two main categories [1].

Category 1 - Enhancing the Spectral Efficiency per Area:

In this category, the purpose is to enhance the overall spectral efficiency of the communication. In other words, this corresponds to serving as many users as possible in a given area. Examples of this include Non-Orthogonal Multiple Access (NOMA) techniques which serve many superimposed users using the same resources of frequency, code or time. Also, Massive Multiple Input Multiple Output (MIMO) falls under this category where very large number of antenna elements are used at the base station for enhancing the spectral/energy efficiency [1], [2]. Although NOMA and massive MIMO achieve considerable gains in terms of area spectral efficiency enhancement, they result in large processing latency, an increase in the digital signal processing complexity of the transceiver design, and low energy utilization efficiency [3]. Another scheme that enhances the overall system spectral efficiency is In-Band Full Duplex

[1]Note that only the techniques which propose ways of using the available amount of the wireless spectrum in an efficient manner are given as examples. mm-Wave, for example, is not included since it is related with licensing additional spectrum region.

(IBFD) where a wireless terminal is allowed to transmit and receive simultaneously in the same frequency band; however this technique suffers from self-interference, complex receiver design and incompatibility with current wireless devices and standards [4].

Category 2 - Enhancing the Spectral Efficiency per User/Device:

Unlike the schemes such as NOMA and massive MIMO which focus on increasing the spectral efficiency by serving as many users as possible per area, another promising research direction studies ways for increasing the spectral efficiency per user/device. This is possible through the use of multi-dimensional OFDM modulations where parameters related to the OFDM waveform are explored as new dimensions for carrying extra information. This is a novel research direction in which new modulation formats are being developed where data is not sent only through the classical symbol constellations (i.e., typically Phase Shift Keying (PSK) or Quadrature Amplitude Modulation (QAM)) but also some of the data is transmitted through some additional dimensions such as the index of the active subcarriers in an OFDM block, the number of the active subcarriers in the block, ..etc.
It is important to note that this does not result in any waste in the resources (bandwidth) specifically devoted to the exploration of these additional dimensions.
In this scope, the list of explored dimensions can be summarized as follows:

1. **Index:** The index family is one of the most studied dimensions. In this category, the following schemes have been proposed:
    - *SM-OFDM:* Spatial Modulation OFDM (SM-OFDM) was proposed in [5] where the indices of the active antennas are used a an additional dimension for sending extra data.
    - *SIM-OFDM:* SIM-OFDM (Subcarrier Index Modulation OFDM) was proposed in [6] where the indices of the active subcarriers in an OFDM block are explored for conveying extra data bits.
    - *OFDM-IM:* OFDM with index modulation was proposed in [18] which is similar to SIM-OFDM as it explores the indices of the active subcarriers inside the OFDM block for sending additional data bits.
2. **Number:** *OFDM-SNM* (OFDM with Subcarrier Number Modulation) was proposed in [8] where the authors studied the use of the number of the active subcarriers, rather than the index, as a new dimension for sending more data bits.
3. **Gap:** Authors in [9] proposed a technique called *OFDM-SGM* where the they study the gap between active subcarriers in an OFDM waveform as a new dimension for transmitting extra information bits.
4. **Shape:** *OFDM-PSM* short for OFDM-pulse superposition modulation was studied extensively in the literature, in which the pulse shape is used as an extra dimension for data transmission [10].
5. **Power:** We proposed *OFDM-SPM* for doubling the spectral efficiency per device in [11], [12]. *OFDM-SPM* manipulates the power of the subacarriers in an

OFDM block for transmitting an additional stream of data embedded with the classically modulated stream, resulting in doubling the spectral efficiency per receiving node.

2.1.2 Direction 2 / Non-Coherent Modulation Formats

Another promising solution for reducing the complexity and thus enhancing power saving in future systems is the use of non-coherent modulation formats which, unlike coherent systems where very expensive phase estimations are carried out, do not require the knowledge of the the phase of the transmitted signal during demodulation [13], [14].
Since OFDM is the preferred waveform for current communication systems due to its robustness against multipath fading, several OFDM-based non-coherent formats have been developed. Particularly, self-heterodyne OFDM (self-het OFDM) [15] has been proposed as a non-coherent OFDM technique that provides immunity to frequency offset and phase noise. The performance analysis for self-het OFDM was carried out in additive white Gaussian (AWGN) environment as well as in frequency selective channels and the following disadvantages were concluded: (1) in terms of spectral efficiency, it allows maximum utilization of only 50% of the spectrum for communication; (2) the local carrier transmission uses almost half of the transmit power; (3) during the self-mixing process, inter-modulation distortions are exhibited at the receiver[16].
Another technique termed as self-coherent OFDM [17] was proposed, which also adopts a non-coherent design. In [17], it was shown that the additional phase noise (PN) introduced by under-sampling down-conversion in self-het OFDM can be substantially reduced with self-coherent demodulation. Although self-coherent OFDM provides both a better bit error rate and spectral efficiency than self-het OFDM, the maximum utilization of the available spectrum is approximately 80%.
Non-coherent OFDM with index modulation (OFDM-IM) [18] has also been proposed as a non-coherent version of OFDM-IM which conveys data through the indices of the active subcarriers of the OFDM symbol; however, this scheme has also provided worse spectral efficiency than conventional OFDM-IM, depending on the coherence time of the channel.

2.1.3 Non-Coherent OFDM-SPM (NC-OFDM-SPM)

In the sections above, we have discussed:

1. the contribution of multi-dimensional OFDM modulations in enhancing the spectral efficiency per device.

2. the use of non-coherent modulations in the design of future wireless systems as a solution for the requirement of reducing complexity and thus latency of the communication.

In this chapter, we propose and study the performance of a technique which integrates both of these research ideas in its design. The proposed technique is termed as Non-Coherent OFDM with Subcarrier Power Modulation (NC-OFDM-SPM) and provides

the following benefits, through the combination of multi-dimensional OFDM modulations and non-coherent structures utilization.

1. *Doubling the spectral efficiency per device:* NC-OFDM-SPM explores the power of the subcarriers inside an OFDM block as an additional dimension for data transmission, where data is conveyed through two dimensions: the classical modulation scheme (i.e., here DPSK is used) and through the explored additional dimension.
   In particular, the choice of the power as an additional dimension for modulating the OFDM signal ensures doubling the spectral efficiency since all the subcarriers in the OFDM block are used. This is unlike some of the mentioned dimensions (index for example) where only the active subcarriers in the block are used, thus reaching only a partial enhancement of the spectral efficiency.
   Fig.2.1 illustrates this fact and shows that NC-OFDM-SPM represents to OFDM what OFDM represents to conventional FDM (Frequency Division Multiplexing). Compared to FDM, OFDM saves bandwidth through the introduction of the orthogonality principle between the subcarriers and thus saving the bandwidth which was dedicated for the purpose of guard band intervals. Similarly, compared to OFDM, OFDM-SPM saves half the bandwidth required by conventional OFDM (i.e., and twice that of FDM) due to the exploration of the power as an additional dimension on the y-axis. This explored dimension is a virtual dimension and has no bandwidth solely devoted for its exploration. Due to this 2-D setup of OFDM-SPM, for transmitting the same number of bits, OFDM-SPM would only require half the number of subcarriers that conventional OFDM would normally require for this transmission.

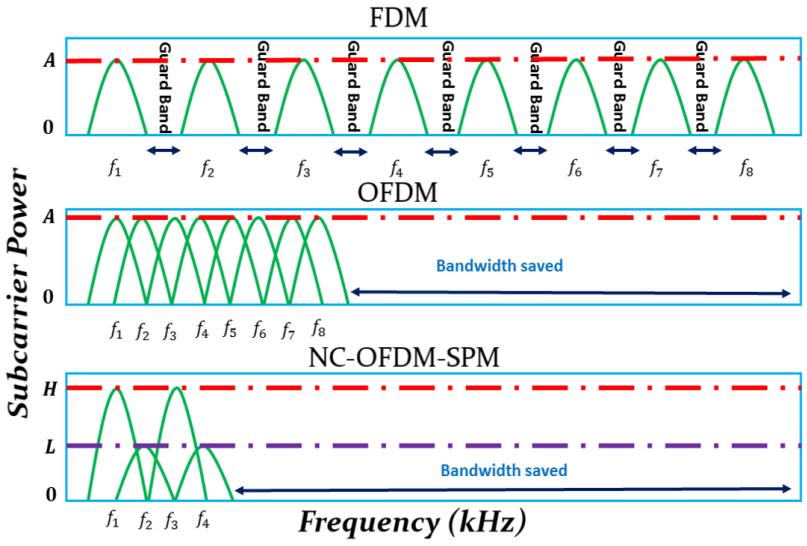

Figure 2.1: NC-OFDM-SPM compared to Conventional OFDM and FDM.

2. *Low-complexity through completely non-coherent communication:* NC-OFDM-SPM uses two types of modulation/demodulation in its design:

   - differential encoding and decoding through the use of DPSK for modulating one sub-stream of data.

- subcarrier power modulation is used for modulating the second sub-stream of data. At the transmitter, the power of the subcarrier is set to high (H) and low (L) while in the receiver this sub-stream is demodulated from the received joint stream through threshold detection.

Both operations ensure complete non-coherence in the proposed architecture, yielding a lower complexity for this design.

In this chapter, we study different aspects of NC-OFDM-SPM. Its performance is investigated and demonstrated in terms of mathematical derivations and extensive computer simulations.

2.2 System Model and Preliminaries

In this section, the internal architecture of the transmitter and the receiver of NC-OFDM-SPM is discussed.

2.2.1 Transceiver Design

Transmitter of NC-OFDM-SPM

The transmitter of NC-OFDM-SPM is shown in Fig.2.2. As shown in Fig.2.2, the in-

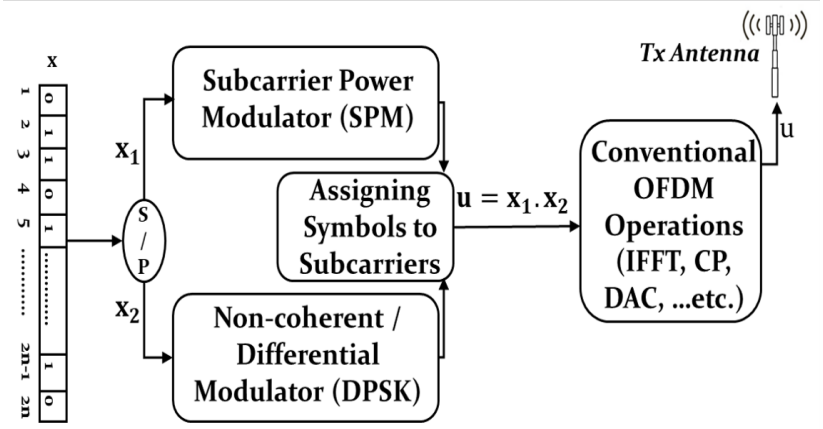

Figure 2.2: Transmitter of NC-OFDM-SPM

coming data stream $\mathbf{x}$ is divided into two sub-streams $\mathbf{x_1}$ and $\mathbf{x_2}$ of equal length where one of the sub-streams ($\mathbf{x_2}$) is modulated using classical differential phase shift keying (DPSK) and the other stream ($\mathbf{x_1}$) is modulated through the subcarrier power modulation. Subcarrier power modulation corresponds to a 2-level power modulation where, depending on the incoming data, the subcarrier power is set to high (H) if the incoming data bit is $'1'$ or set to low if the incoming data bit is $'0'$. The values of (H) and (L) depend on the power policy used. In the next section a detailed discussion on the power policies is performed. After separate modulations the two sub-streams are joined into a combined stream which is then passed through the IFFT block and the rest of the operations of conventional OFDM. In this combined stream both the DPSK symbols and the power symbols are embedded.

Signal Constellation

The proposed mapping scenario results in the constellation diagram of Fig.2.3 where the binary pair $'ij'$ denotes a power subcarrier (i.e., low if $'i' = 0$ and high if $'i' = 1$) carrying a bit $'j'$ modulated by differential BPSK.

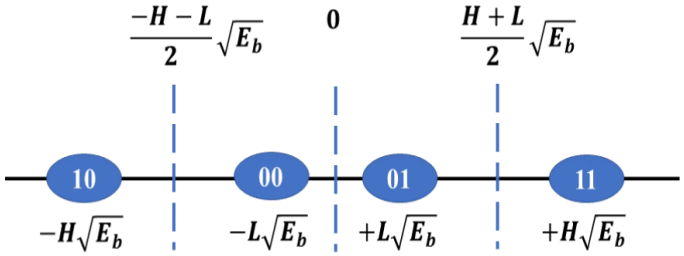

Figure 2.3: Constellation diagram of NC-OFDM-SPM.

Channel

This study considers a frequency selective fading Rayleigh channel with L number of exponentially decaying taps, denoted by $h = [h_0, h_1, h_2, ..., h_{L-1}]$. The received signal can be written as:

$$y = x \otimes h + n \tag{2.1}$$

where the $\otimes$ denotes the convolution operator. The symbols x, y, h are vectors representing the transmitted time domain samples, received samples in the time domain, and the channel impulse response. n represents the AWGN noise distributed with zero mean and variance equal to N_0, $n \sim \mathcal{N}(0, N_0)$. Additionally, the channel is slowly varying in time such that it is assumed to be constant for multiple OFDM symbols duration before it changes independently in the subsequent time intervals.

Receiver of NC-OFDM-SPM

The receiver diagram of NC-OFDM-SPM is shown in Fig.2.4. The individually modulated data sub-streams $\mathbf{x_1}$, $\mathbf{x_2}$ are demodulated from the incoming combined stream u. The data sub-stream $\mathbf{x_1}$ is decoded through the subcarrier power demodulator where the original power levels are recovered by comparing the received signal power (square of the amplitude of the received data) to a threshold T defined as the midpoint between the high and low levels (H and L).

$$T = (\frac{H+L}{2})^2 \tag{2.2}$$

Thus, if at the i^{th} position in the received symbol $\|\mathbf{x_1(i)}\|^2 \leq T$, then $\mathbf{x_1(i)} = L$, else $\mathbf{x_1(i)} = H$. Then, as we know from the SPM mapping in the transmitter, $H \Rightarrow 1, L \Rightarrow 0$.

The data sub-stream $\mathbf{x_2}$ is demodulated through the conventional DPSK demodulation process according to the phase difference between the received symbols.

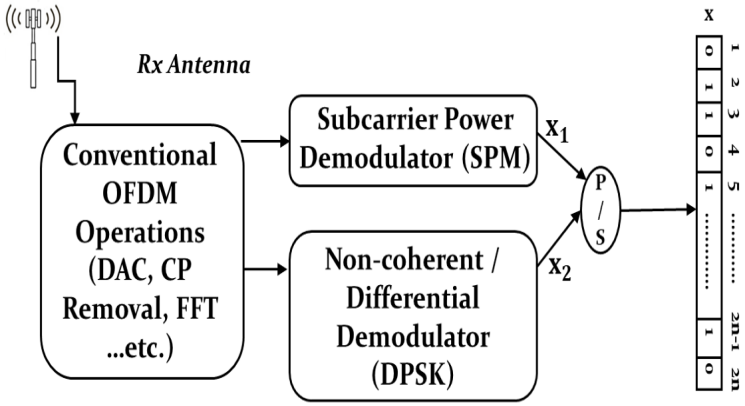

Figure 2.4: Receiver of NC-OFDM-SPM.

2.3 Performance Analysis

In this section, the performance analysis of NC-OFDM-SPM is presented. First, a short discussion on the merits of the non-coherence property of this design is done. Then, the bit error rate (BER) analysis is performed, the formulated power policies are presented and the spectral efficiency performance is discussed. Finally, the Peak to Average Power Ratio (PAPR) is discussed.

2.3.1 Non-Coherence of NC-OFDM-SPM

As can be seen from the transmitter and receiver diagrams of NC-OFDM-SPM, the design relies on two operations:

1. *Subcarrier power modulation/demodulation:* This is a non-coherent operation since the phase is not used in the detection of the received bits where only the received signal power is measured and compared to the defined threshold T for recovering the original power levels.

2. *Differential modulation/demodulation:* This operation is also a non-coherent modulation where no reference phase signal is used; the transmitted signal itself is used as a reference signal as well. The phase is embedded in the difference between the received symbols not in the symbols themselves.

As such, since both operations employed in the design of the proposed technique are non-coherent, NC-OFDM-SPM can be considered as a non-coherent technique.
The non-coherence of the design implies the following merits:

- No need for synchronization because both operations are non-coherent, thus getting rid from phase recovery circuits which are regarded as a main source of complexity and latency in coherent systems.

- low design complexity due to the simplicity of the used operations (i.e., threshold-based detection & differential detection) which guarantees a low-latency transmission.

It is important to note that with this simple transceiver design, NC-OFDM-SPM-DPSK surpasses some of the known schemes, which explore an extra dimension for data transmission such as subcarrier number (OFDM-SNM), subcarrier index (OFDM-IM, SIM-OFDM) which usually employ either a maximum likelihood (ML) detector for optimum performance, or a log likelihood ratio (LLR) detector for reduced complexity [20].

2.3.2 BER Analysis

As shown in the discussion of the transceiver for NC-OFDM-SPM, a combined stream of data is transmitted. This combined/joint stream includes in it the two independently modulated sub-streams (i.e., through power/DPSK). Let BER_S stand for the probability of error of the joint stream while BER_{PS} and BER_{DS} stand for the error rates for the power sub-stream and the DPSK sub-stream, respectively.
The overall error probability of the scheme can be defined as the average of the probability of the detection of both blocks (power/DSPK).

$$BER_S = \frac{BER_{DS} + BER_{PS}}{2} \tag{2.3}$$

Derivation of BER_{DS}:

The bit error rate of conventional OFDM with binary DPSK in Rayleigh [21], given in the equation below, can be taken as the basis for the derivation of the bit error rate expressions for the DPSK stream.

$$BER_{Differential\ OFDM-BPSK} = \frac{1}{2\left(1 + \frac{E_b}{N_0}\right)} \tag{2.4}$$

where, $\frac{E_b}{N_0}$ denotes the signal to noise ratio.
BER_{DS} is the same as the bit error rate of conventional OFDM with DPSK expressed by Eq.(2.4) where the only difference is that, in our case, since the power stream is embedded with the DPSK stream, the high and low levels have an effect on the detection of the DPSK curve as they change the euclidean distances between the symbols. This effect can be accounted for in Eq.(2.4) as follows:

$$BER_{DS} = \frac{BER_H + BER_L}{2} \tag{2.5}$$

where,

$$BER_H = \frac{1}{2\left(1 + H^2 \frac{E_b}{N_0}\right)} \tag{2.6}$$

$$BER_L = \frac{1}{2\left(1 + L^2 \frac{E_b}{N_0}\right)} \tag{2.7}$$

represent, respectively, the effect of the high and low power levels on the detection of the DPSK-modulated bit stream from the joint received stream.

Derivation of BER_{PS}:

The noise and the multipath effects can cause a high power subcarrier H to be detected as a low power subcarrier L, or vice versa. As shown in Fig.2.5 and as explained from the system model, the detection of the power stream is based on a comparison with the detection threshold defined as the midpoint between the high and low levels.
As presented in Fig.2.5, the transition from high to low represented by the red arrow corresponds to a minimum euclidean distance of $d_{H\rightarrow L} = |H - \frac{H+L}{2}| = \frac{H-L}{2}$. The erroneous transition from low to high is indicated by the blue arrow and corresponds to crossing a minimum euclidean distance of $d_{L\rightarrow H} = |\frac{H+L}{2} - L| = \frac{H-L}{2}$. Similar to the

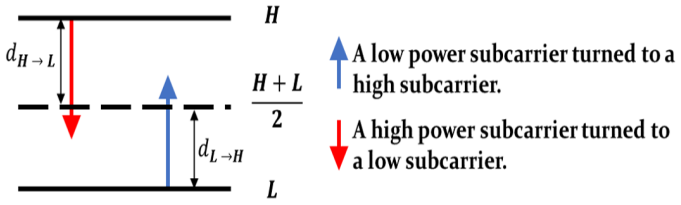

Figure 2.5: Erroneous detection of the power stream.

derivation of the bit error rate of the DPSK stream above, the power stream can also be derived by accounting for the euclidean distance changes introduced by the high and low levels in the expression of the classical 2-level pulse amplitude modulation.
The general expression for M-level pulse amplitude modulation, in AWGN, is given in [22] as:

$$BER_{M-PAM} = 2(1 - \frac{1}{M})Q_\alpha(\frac{d}{\sigma}) \tag{2.8}$$

where d is the decision distance, σ is the standard deviation. $Q_\alpha(.)$ is the generalized Gaussian Q function, defined in [23], for $x \geqslant 0$ as:

$$Q_\alpha(x) = \frac{\alpha\Lambda_0}{2\Gamma(1/\alpha)} \int_x^\infty \exp(-\Lambda_0^\alpha t^\alpha)\, dt \tag{2.9}$$

where, $\Gamma(.)$ is the Gamma function and $\Lambda_0 = \sqrt{\frac{\Gamma(3/\alpha)}{\Gamma(1/\alpha)}}$.
Note that for $M = 2$, the expression defined by Eq.(2.8) becomes:

$$BER_{2-PAM} = Q_\alpha(\frac{d}{\sigma}) \tag{2.10}$$

which is the same as the bit error rate for BPSK, in AWGN, as defined in [22]. Thus, we can take the BPSK expression as our basis for the derivation of BER_{PS} by integrating $d_{H\rightarrow L}$ and $d_{L\rightarrow H}$ in it to account for the effect on the distance change between the symbols introduced by the high and low levels. The expression for OFDM-BPSK, in Rayleigh, is given as [32]:

$$BER_{OFDM-BPSK,\ Rayleigh} = \frac{1}{2}\left(1 - \sqrt{\frac{\frac{E_b}{N_0}}{1 + \frac{E_b}{N_0}}}\right) \tag{2.11}$$

where the Euclidean distance between the symbols is a function of ratio between the energy of the symbols and noise variance (i.e., $\frac{E_b}{N_0}$). Taking Eq.(2.11) as a basis, and

assuming that both transitions in Fig.2.5 are equally likely to happen, the theoretical BER expression of the power stream can be written as:

$$BER_{PS} = \frac{1}{2}BER_{H\to L} + \frac{1}{2}BER_{L\to H} \tag{2.12}$$

where,

$$BER_{H\to L} = \frac{1}{2}\left(1 - \sqrt{\frac{(d_{H\to L})^2\frac{E_b}{N_0}}{1+(d_{H\to L})^2\frac{E_b}{N_0}}}\right) \tag{2.13}$$

$$BER_{L\to H} = \frac{1}{2}\left(1 - \sqrt{\frac{(d_{L\to H})^2\frac{E_b}{N_0}}{1+(d_{L\to H})^2\frac{E_b}{N_0}}}\right) \tag{2.14}$$

where, $BER_{H\to L}$ denotes the BER expression for detecting a high power level as a low power level, and $BER_{L\to H}$ denotes the BER expression for detecting a low power level as a high power level.

2.3.3 Power Policies

Due to the exploration of the high and low power pattern as an extra data-carrying dimension, the proposed scheme combines two data streams; a stream of data modulated by DPSK and another modulated by the power levels. As such, for sending the same number of data bits using conventional OFDM, NC-OFDM-SPM would require half the number of subcarriers compared to OFDM as shown in Fig.2.6. This difference between NC-OFDM-SPM and conventional OFDM leads to the formulation of different power policies for NC-OFDM-SPM including power saving policy and power reassignment policy.

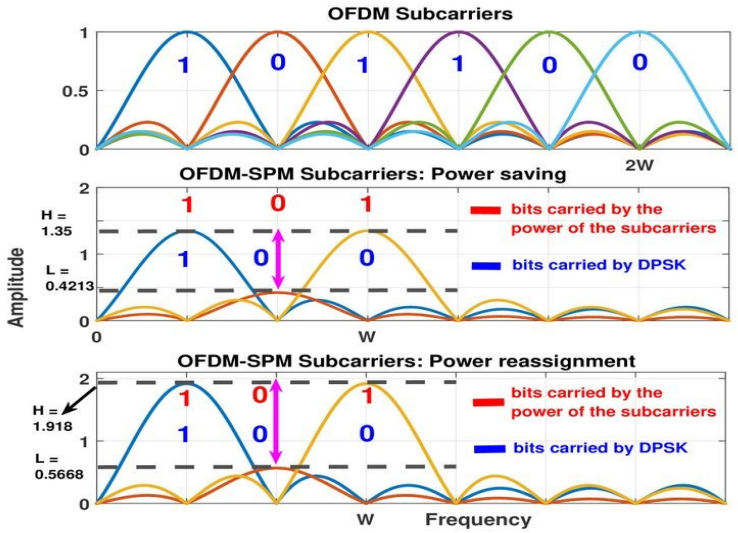

Figure 2.6: Exemplary transmission: NC-OFDM-SPM vs Conventional OFDM.

Power Saving Policy (PSP)

In this policy, half the transmit power is saved by NC-OFDM-SPM compared to OFDM since NC-OFDM-SPM-DPSK uses only half the number of subcarriers required by conventional OFDM for transmitting the same number of bits. The values of the high and low levels corresponding to this case can be defined with the following equation:

$$\frac{H^2 + L^2}{2} = E_b \tag{2.15}$$

where it is shown that the high and low levels used for subcarrier power modulation are chosen such that the average energy per bit does exceed that of binary phase shift keying where the bit energy is E_b.
This policy is developed for serving the demands of communication devices with low-power requirements.

Power Reassignment Policy (PRP)

The saved power can be reassigned to the transmit subcarriers to enhance the reliability performance of the proposed scheme. In the power reassignment policy, the power levels (H, L) can be defined using the following equation:

$$\frac{H^2 + L^2}{2} = 2E_b \tag{2.16}$$

where the factor 2 in the right side of Eq.(2.16) expresses the reassignment of the saved power to the transmit subcarriers. The reassignment operation can be done in many ways, where every pair of power levels (H, L) corresponds to some effect on the bit error rate of the individual streams $(i.e., BER_{DS}$ & $BER_{PS})$. More specifically, we treated two special cases of reassignment each corresponding to a different optimization problem.

1. *Case 1 / PRP for Optimized Overall Performance(PRP-OOP):*
   In this case, the average performance is optimized. This corresponds to finding the high and low pair (H, L) that makes the average bit error rate curve (i.e., average of the BER curve corresponding to the detection of the power bits and the BER curve corresponding to the detection of the DPSK modulated bits) attains the optimal (i.e., minimum possible) BER performance.

2. *Case 2 / PRP for Achieving the Coherent Performance of OFDM (PRP-ACP):*
   This case is concerned with a classical problem in the literature which is the trade-off between coherent and non-coherent modulations. As it is known from the literature, non-coherent systems are less complex compared to coherent systems; however they perform worse than their coherent counterparts in terms of reliability. We have seen from the above section that the proposed design is totally non-coherent. Moreover, the proposed design is more flexible compared to conventional modulation formats where only one dimension is explored for modulating the transmitted data and thus the mentioned trade-off can be explored in the light of this modulation flexibility. The mentioned trade-off can

be solved by the following settings of NC-OFDM-SPM:

$$(S_{PRP-ACP}) \begin{cases} BER_{DS} = BER_{Coherent\ OFDM-BPSK} \\ No\ constraint\ on\ BER_{PS} \end{cases} \tag{2.17}$$

, where the first equation in $(S_{PRP-ACP})$ corresponds to setting the DPSK stream to match the performance of coherent OFDM-BPSK, while the second equation corresponds to setting the power curve constraint-free for allowing a degree of freedom in the optimization.

2.3.4 Spectral Efficiency

Spectral efficiency is a necessary metric for evaluating the performance of wireless systems. In particular, since the present and future are characterized with a massive emergence of wireless devices, serving these collection of devices with techniques that can respond to their day per day growing demands is really an urgent need. In this regard, NC-OFDM-SPM is capable of doubling the spectral efficiency per device/user as shown in Fig.2.7. This is due to the fact that a single subcarrier in NC-OFDM-

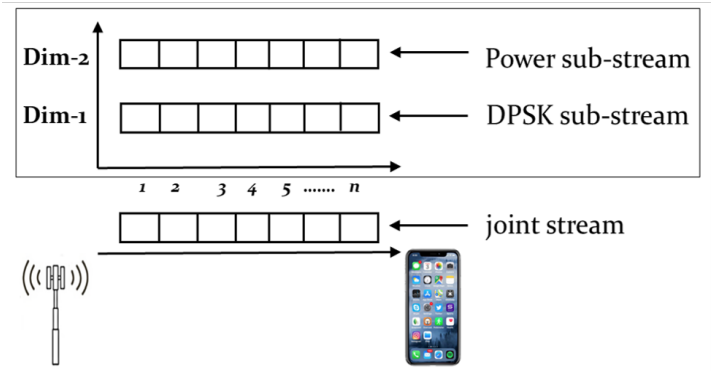

Figure 2.7: NC-OFDM-SPM doubles the spectral efficiency per device.

SPM carries two bits, while a conventional OFDM with BPSK/DPSK is capable of carrying only one bit per subcarrier. This shows that OFDM-SPM doubles the data rate, compared to a conventional OFDM system using BPSK/DPSK. It is important to note that among the multi-dimensional OFDM schemes that were mentioned for enhancing the spectral efficiency per user/device, only the power dimension leads to doubling the spectral gain due to the utilization of all the subcarriers in the block for data transmission, while all the other dimensions (index, number, ... etc) are able to reach only a partial improvement of the spectral efficiency since they convey data using only the active subcarriers in the block.

2.3.5 Peak to Average Power Ratio (PAPR)

The Peak to Average Power Ratio (PAPR) metric is defined for a transmit signal x, as its name implies, as follows:

$$PAPR[x(t)] = \frac{Maximum\ Instantaneous\ Power}{Overall\ Average\ Power} = \frac{\max[\|x(t)\|^2]}{\mathbb{E}[\|x(t)\|^2]}, 0 \leq t \leq N \tag{2.18}$$

where $\mathbb{E}[.]$ denotes the expectation operator. The peak to average power ratio (PAPR) is an important metric for assessing the performance of all communication systems based on OFDM. Unlike single carrier systems, OFDM systems are characterized with high PAPR values due to the reason that the transmit signals in OFDM are the result of the addition of many subcarriers using the IFFT process. The high PAPR is regarded as one of the main disadvantages of OFDM systems as it leads to decreasing the efficiency of the power amplifier. As such, PAPR is an important performance for any technique based on OFDM where it is important to investigate the behaviour of the PAPR and if it induces any amplification or reduction compared to conventional OFDM. PAPR simulations of the proposed design, under different power policies, are given in the next section.

2.4 Simulation Results

In this section, the simulation results of the proposed design are presented. All the simulations were obtained using the MATLAB simulation environment. The list of simulation parameters is indicated in Table 2.1.

Table 2.1: NC-OFDM-SPM / Simulation Parameters

Parameter	**Value**
Modulation type	DPSK (M = 2)
IFFT / FFT size	64
Subcarriers for data *n*	52
Symbols allocated for cyclic prefix	16
Number of inactive sub-carriers for out of band emission	12
Number of OFDM symbols	2×10^4
Channel model	Rayleigh
Multipath channel delay samples locations	[0 3 5 6 8]
Multipath channel tap power profile (dBm)	[0 -8 -17 -21 -25]

2.4.1 Power Saving Policy (PSP)

The power levels in the simulation of this case are defined as in Eq.2.15, and were found as $H = 1.35$ and $L = 0.4213$. These values ensure obtaining the best performance possible with NC-OFDM-SPM while saving 50% of the transmit power compared to conventional OFDM.
In Fig.2.8, bit error rate simulations for the power saving mode are displayed. As can be seen from this plot, NC-OFDM-SPM exhibits some BER degradation compared to conventional OFDM; however it surpasses conventional OFDM through doubling the spectral efficiency as displayed in Fig.2.9 while saving 50% of the transmit power.
In Fig.2.10, the peak to average power ratio simulations of the proposed NC-OFDM-SPM versus conventional OFDM with DPSK are displayed where it can be observed that the proposed design does not add further degradation over (conventional OFDM)'s PAPR.

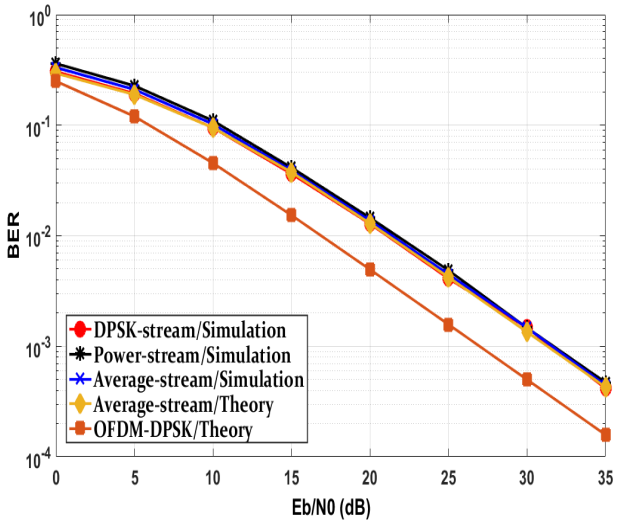

Figure 2.8: Bit error rates for NC-OFDM-SPM in the PSP mode.

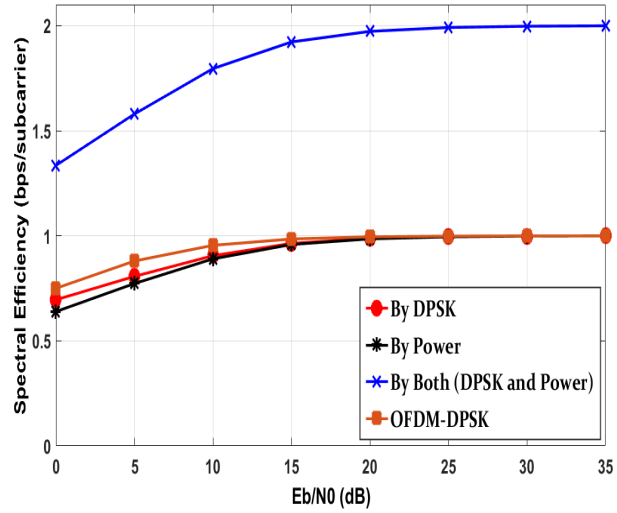

Figure 2.9: Data rates for NC-OFDM-SPM in the PSP mode.

2.4.2 Power Reassignment Policy (PRP)

In this section, the power reassignment mechanism results are presented. It is to be noted that the power reassignment is an optimization problem where the goal is to find the values (H, L) which correspond to a specific performance level (i.e., measured through BER). In regard, two special cases were treated as explained in section 2.3.3.

Case 1: PRP-OOP, PRP for Optimized Overall Performance

This section is concerned with the case where the optimal average BER is obtained. This corresponds to finding the subcarrier power levels H and L such that the average error rate BER_S defined in Eq.(2.3) achieves the minimum possible level of error. The values for the high and low power levels specific to this optimization were found as: $(H, L) = (1.918, 0.5668)$.

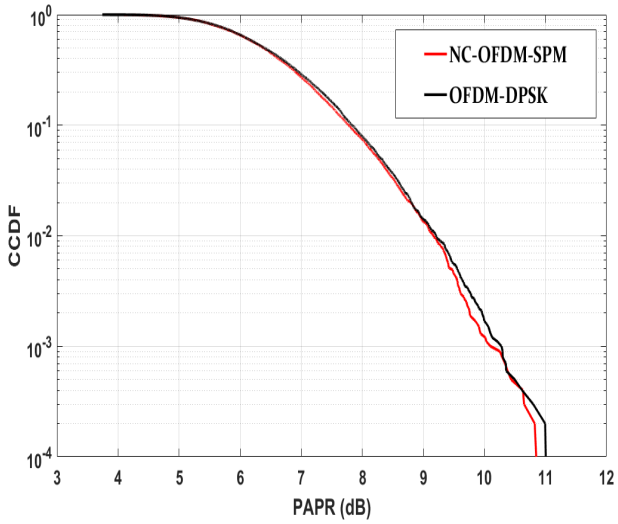

Figure 2.10: PAPR of NC-OFDM-SPM in the PSP mode.

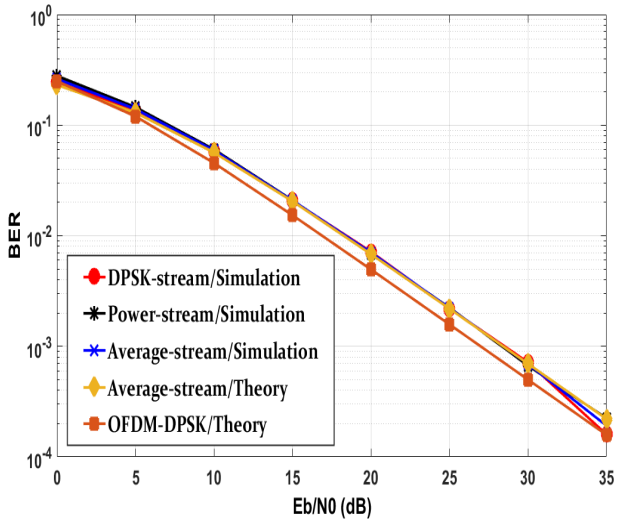

Figure 2.11: Bit error rates for NC-OFDM-SPM in the PRP-OOP mode.

In Fig.2.11, the bit error rate simulations of this case are displayed. It can be seen that the reassignment of the saved power to the transmit subcarriers increases the reliability compared to the power saving mode; however a slight deterioration in the BER corresponding to this case is observed compared to conventional OFDM with DPSK. However, NC-OFDM-SPM surpasses conventional OFDM in terms of data rate as shown in Fig.2.12 where the proposed design achieves doubling the spectral gain per device compared to conventional OFDM.

In Fig.2.13, the PAPR of NC-OFDM-SPM, under the PRP-OOP mode, is compared to conventional OFDM with DPSK. It can be seen that the proposed design attains slightly lower PAPR values compared to conventional OFDM-DPSK.

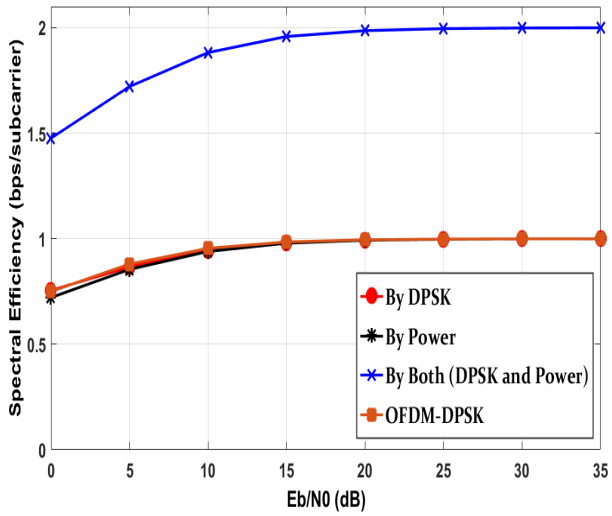

Figure 2.12: Data rates for NC-OFDM-SPM in the PRP-OOP mode.

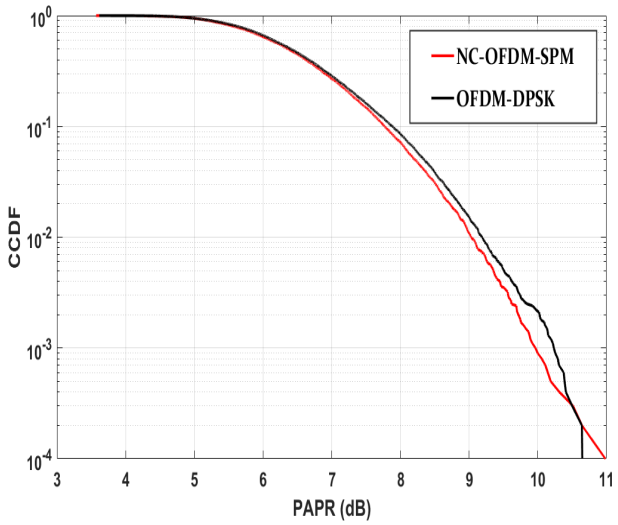

Figure 2.13: PAPR for NC-OFDM-SPM in the PRP-OOP mode.

Case 2: PRP-ACP, PRP for Achieving the Performance of Coherent OFDM-BPSK

As highlighted in section 2.3.3, this case was treated because it deals with a problem that is classical in communication systems which is the trade-off between coherent and non-coherent systems.
The optimal low (L) and high (H) power levels satisfying $(S_{PRP-ACP})$ are found by the following iterative algorithm.

1. By setting H to an arbitrary value, the corresponding value for L can be found, by using Eq.(2.16), as:
$$L = \sqrt{4E_b - H^2} \tag{2.19}$$

2. For every choice of L and H defined according to Eq.(2.19), the error function corresponding to the difference between the proposed non-coherent stream and

the target coherent OFDM-BPSK stream, defined in $(S_{PRP-ACP})$, is calculated

$$\epsilon = BER_{DS} - BER_{Coherent\ OFDM-BPSK} \tag{2.20}$$

where the goal is to minimize the error between the two curves.
The expression $BER_{Coherent\ OFDM-BPSK}$ is the bit error rate for coherent conventional OFDM-BPSK, in Rayleigh, and is given in [21] as:

$$BER_{Coherent\ OFDM-BPSK} = \frac{1}{2}\left(1 - \sqrt{\frac{\frac{E_b}{N_0}}{1+\frac{E_b}{N_0}}}\right) \tag{2.21}$$

3. Steps 1) and 2) are repeated for numerous (H, L) pairs and the obtained error is recorded. The smallest error is found for the following (H, L) pair:

$$H = 1.732,\ L = 1 \tag{2.22}$$

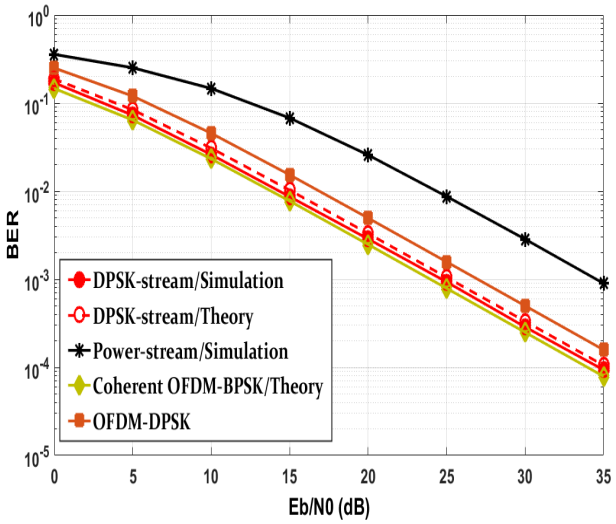

Figure 2.14: Bit error rates for NC-OFDM-SPM / PRP-ACP.

Bit error rates corresponding to this case are displayed in Fig.2.14, where it is shown that NC-OFDM-SPM in the PRP-ACP mode surpasses the performance of non-coherent conventional OFDM with DPSK and reaches the performance of coherent OFDM with BPSK. Moreover, in Fig.2.15 it can be seen that the proposed design, which is a non-coherent design, reaches the performance of coherent OFDM-BPSK with a very slight error.
It is to be noted that this coherent performance is only attained by the DPSK stream of NC-OFDM-SPM while the power stream experiences some performance degradation compared to conventional OFDM. This power stream is an additional benefit where it can be allocated for a user application which does not require ultra-reliability.
Furthermore, NC-OFDM-SPM surpasses conventional OFDM by doubling the spectral efficiency as shown in Fig.2.16.
In Fig.2.17, the PAPR results are displayed where it can be seen that, under PRP-ACP mode, NC-OFDM-SPM achieves the same performance as conventional OFDM with DPSK.

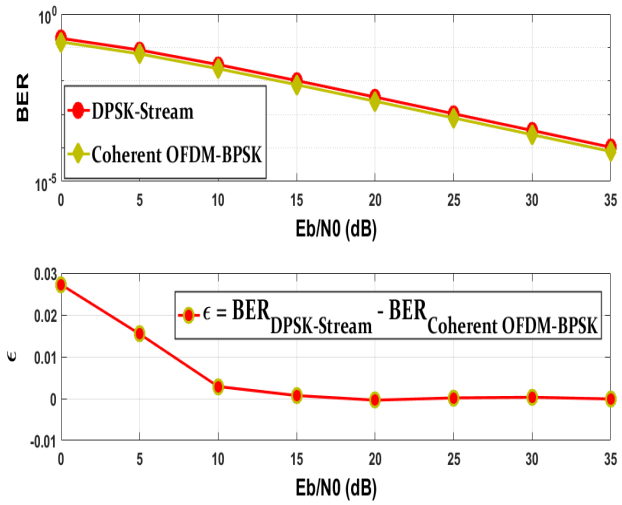

Figure 2.15: Error plot for NC-OFDM-SPM / PRP-ACP, defined as in Eq.(2.20).

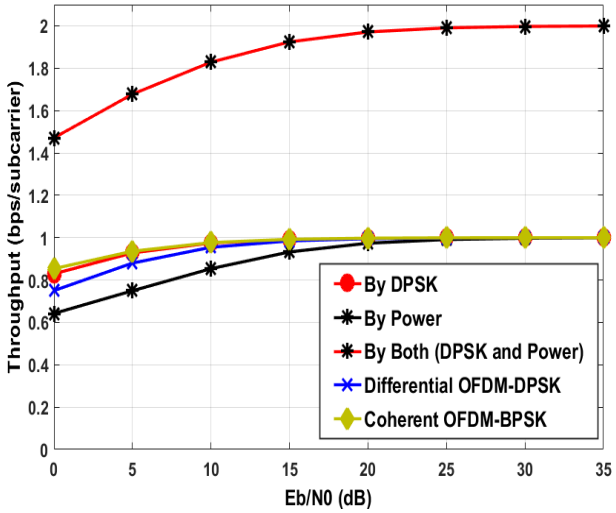

Figure 2.16: Data rates for NC-OFDM-SPM in the PRP-ACP mode.

2.5 Conclusion

In this chapter, Non-Coherent OFDM with Subcarrier Power Modulation (NC-OFDM-SPM) was proposed and studied as a non-coherent multi-dimensional OFDM modulation format. The proposed design explores the power of the subcarriers in an OFDM block as an additional data dimension where data is transmitted through both the classical DPSK constellation symbols and through the the subcarriers' power difference. Due to the exploration of the power as an additional dimension, NC-OFDM-SPM is capable of doubling the spectral efficiency per receiving node where, in the transmitted data stream, it embeds two independently modulated streams of data; a stream modulated through the classical DPSK and a second one modulated through subcarrier power modulation. In this way, NC-OFDM-SPM carries two bits per subcarrier thus it is doubling the spectral efficiency compared to a conventional OFDM system using binary modulation which carries only one bit per subcarrier.

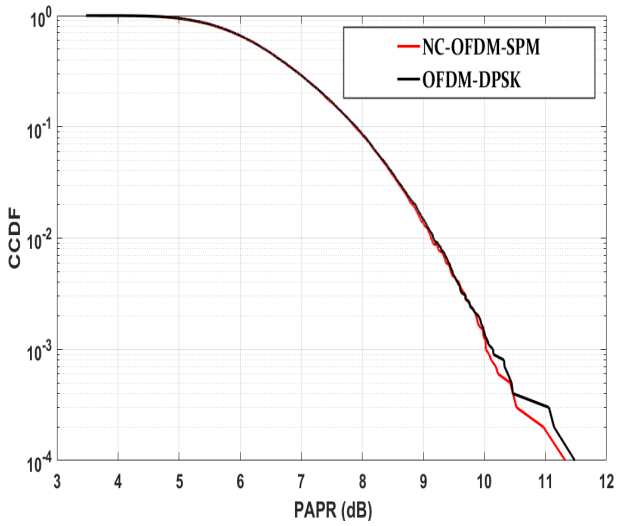

Figure 2.17: PAPR for NC-OFDM-SPM in the PRP-ACP mode.

Moreover, due to its complete non-coherence (i.e., where differential and threshold detection are used for detecting the transmitted streams), NC-OFDM-SPM is characterized by low-complexity and thus lower latency.
Furthermore, different power policies where formulated for this design including power saving policy where half the transmit power is saved by NC-OFDM-SPM compared to conventional OFDM for matching the requirement of low power applications, and the power reassignment mode where the saved power is reassigned to the transmit subcarriers for enhancing the reliability of the transmission.

Chapter 3

Multi-User Auxiliary Signal Superposition Transmission (MU-AS-ST)

3.1 Introduction

3.1.1 Overview of Power Domain Non-Orthogonal Multiple Access (PD-NOMA)

For a better usage of the spectrum allocated for wireless communications, multiple access techniques have been used since the first generation (i.e., $1G$) of wireless communication systems for serving multiple users through the same frequency, time or code resources simultaneously, as shown in table 3.1 for various wireless generations. Currently used $4G - LTE$ systems use orthogonal multiple access techniques, however this kind of techniques were found incapable of addressing the challenging requirements of $5G$ networks such as ultra-reliable low latency communications (URLLC), enhanced mobile broadband (eMBB), and massive machine-type communications (mMTC). As an alternative, several Non-Orthogonal Multiple Access (NOMA) based techniques with varying degrees of success in addressing the challenging requirements of $5G$ have been proposed for standardization by both the wireless academia and the wireless industry.

Table 3.1: Multiple Access Techniques for Different Wireless Generations.

Generation	***Multiple Access Technique***
$1G$	**FDMA** (**F**requency **D**ivision **M**ultiple **A**ccess)
$2G$	**TDMA** (**T**ime **D**ivision **M**ultiple **A**ccess)
$3G$	**CDMA** (**C**ode **D**ivision **M**ultiple **A**ccess)
$4G$	**OFDMA** (**O**rthogonal **F**requency **D**ivision **M**ultiple **A**ccess)

In this regard, a particular technique that gained too much interest in the $5G$ literature is power domain NOMA (PD-NOMA) which was considered as a study item in 3GPP (3rd Generation Partnership Project) from release 13 to release 16 under the name Multi-User Superposition Transmission (MUST) [24]. PD-NOMA was chosen

by 3GPP since it has proven very efficient in many aspects when compared to Orthogonal Multiple Access (OMA)-based schemes where PD-NOMA achieves benefits such as high throughput, massive connectivity and coverage, low latency and signaling overhead, and relaxed channel feedback [25].

On the other hand, PD-NOMA was eliminated from the study items of release 17 of the 3GPP community after being investigated thoroughly from release 13 till 16 [24],[26]. Some of the limitations and the shortcomings exhibited by PD-NOMA, which can serve as an explanation for the reason behind its exclusion from the 3GPP study items, after being considered as a study item from release 13 to release 16, can be summarized in the following points:

- *Inefficiency of NOMA in multi-antenna settings:* PD-NOMA exhibits performance degradation when compared to multi-user multiple input multiple output (MU-MIMO) systems. In this regard, authors in [27] have shown that most of the benefits of power domain NOMA are only valid when the results are compared with OMA. Furthermore, in this detailed review, it is shown that both multi-user linear precoding (MU-LP) and MU-MIMO outperform conventional power domain NOMA.

- *Receiver complexity related to the use of SIC:* the main operation in conventional NOMA is the inter-user interference cancellation through SIC performed by near users, however; this comes at the ultimate cost of receiver complexity. The receiver complexity grows with the number of super-imposed users and as such, NOMA would not be a suitable choice for communication setups where massive connectivity and low-complexity are crucial requirements as in the case of internet of things (IoT) communications.

- *In-applicability in general scenarios due to constrained users' superposition:* one of the limitations of NOMA is the deficiency of working in power-balanced scenarios as it requires a significant path-loss / channel difference between paired (or super-imposed) users. This necessitate having a user near to the base station (i.e., strong channel) and another user far from the base station (i.e., weak channel). Consequently, this limits the applicability of NOMA in general scenarios, where two users may have the same path-loss due to being located at a similar distance from the base station (BS).

- *Security of the NOMA waveform:* Another concern is the security of the NOMA waveform where using SIC for decoding users' data can yield internal eavesdropping risks in the presence of un-trusted users in the superimposed data. Moreover, there is a need for securing NOMA against external eavesdropping [28].

3.1.2 MU-AS-ST as an alternative for PD-NOMA

All the the aforementioned shortcomings of conventional PD-NOMA have motivated the design of novel multiple access alternatives with varying degrees of success in addressing the requirements of future wireless systems.

In this scope, we propose a novel physical layer security based design for effective future multiple access wireless systems. The proposed design makes use of auxiliary

signal superposition where channel-dependent auxiliary signals are added on top of the multiplexed users' signals, which are transmitted from two different antenna sources as shown in Fig.3.1., in such a way that a completely (inter-user interference)-free, secure and reliable transmission is achieved. This chapter is devoted for studying MU-AS-ST

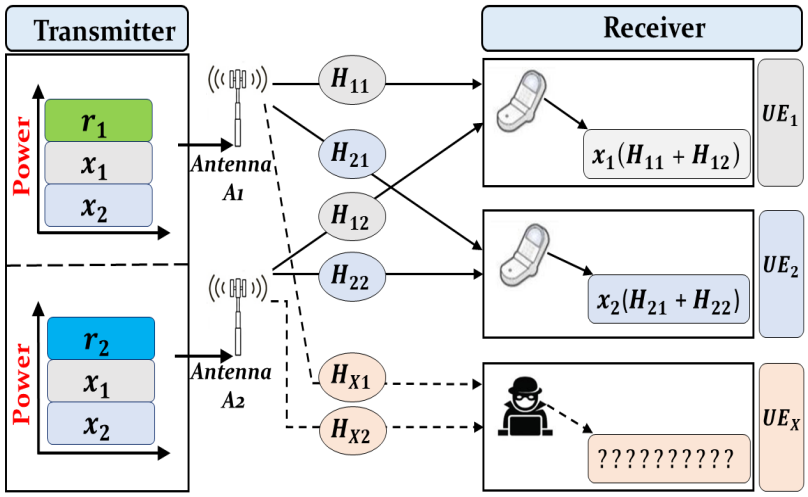

Figure 3.1: General system model of MU-AS-ST.

in depth and proving its capacity in addressing the challenging requirements of future wireless communication systems.
In summary, the contribution points of the proposed design can be presented as follows:

- *Working in general scenarios:* Unlike conventional NOMA where only users having different distance from the base station can be super-imposed, this design works for the combination of any two users regardless of their distances from the base station.

- *Perfect information secrecy against both external and internal eavesdropping:* The design of the auxiliary signals ensures perfect secrecy with zero information leakage to external illegitimate users. Moreover, internal eavesdropping (i.e., in the presence of an untrusted device in the superimposed users) is not possible, due the complete cancellation of all the other signals which do not belong to the receiving node which tries eavesdropping.

- *Reduced receiver complexity & Transmission latency:* Unlike conventional NOMA where successive cancellation at the receiver side leads to a complexity of the system, in this technique the specific design of the auxiliary signals solves this cancellation problem effectively where every device receives it own signal only. Moreover, since the processing performed at the transmitter for designing the auxiliary signals employs diagonal matrices this makes the computational process faster and thus contributes to lowering the latency of the transmission. Furthermore, at the receiver simply a conventional OFDM receiver is used and thus freeing the receiver from any complex processing making from this design a strong candidate for processing-restricted applications such as IoT devices.

3.2 System Model and Preliminaries

The general system model of MU-AS-ST was proposed in Figure 3.1 where its underlying design principles were explained. In this section, we carry on with a more detailed explanation of the internal working mechanisms of the transmitter and the receiver.

3.2.1 Transmitter Design

The design of the proposed technique is based on OFDM. The detailed transmitter of the proposed scheme is shown in Figure 3.2 where the following operations are performed:

- *Symbol modulation:* First, the symbols are modulated using classical Binary Phase Shift Keying (BPSK).
- *Addition of the Auxiliary Signals, (*$\mathbf{r_1}, \mathbf{r_2}$*):* This is the unit responsible for the addition of the specifically designed auxiliary signals to the superimposed data of UE_1 (i.e., $\mathbf{x_1}$) and UE_2 (i.e., $\mathbf{x_2}$). These signals are designed in such a way that the inter-user interference is cancelled and secrecy against both internal (i.e., untrusted legitimate user) and external eavesdroppers is attained.
- *IFFT & CP-Addition:* After the addition of the auxiliary signals, the remaining conventional OFDM operations are performed such as taking the IFFT, adding cyclic prefix (CP), ... etc.

After performing the above operations, the superimposed signals $\mathbf{u_1} = \mathbf{x_1} + \mathbf{x_2} + \mathbf{r_1}$ and $\mathbf{u_2} = \mathbf{x_1} + \mathbf{x_2} + \mathbf{r_2}$ are transmitted from antennas $\boldsymbol{A}_1$ and $\boldsymbol{A}_2$, respectively.

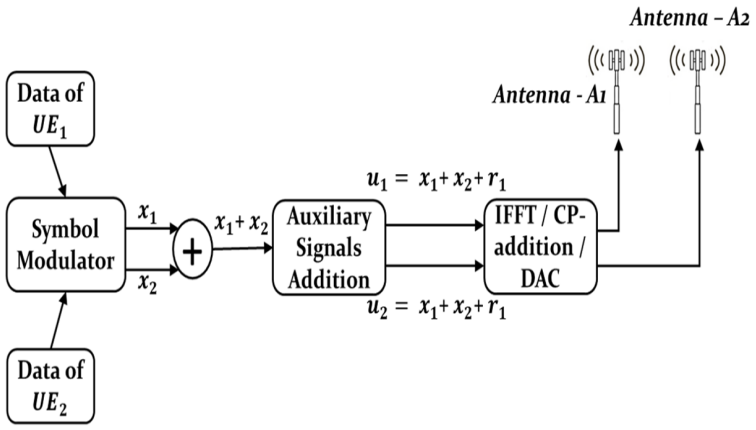

Figure 3.2: Transmitter of MU-AS-ST.

3.2.2 Channel Model

The channel between the transmitter and any receiver is assumed to be a slowly-varying, frequency selective Rayleigh type channel with with L multi-path exponentially decaying taps, denoted by $h_{ij} = [h_0, h_1, ..., h_{L-1}], i \in (1, 2), j \in (1, 2, X)$. As

such, the received symbols in time domain are given as:

$$y_j = (\sum_{i=1}^{2} u_i \otimes h_{ji}) + n_j \tag{3.1}$$

where $\otimes$ represents the convolution operator. h_{ji} stands for the channel impulse response between the antenna $\boldsymbol{A_i}$ and the user equipment UE_j. u_i, and n_j are vectors representing the transmitted time domain samples from antenna $\boldsymbol{A_i}$, and the additive white Gaussian noise, respectively. The noise n_j samples are drawn from a normal distribution with zero mean and variance equal to N_0; $n_j \sim \mathcal{N}(0, N_0)$.
Moreover, it is assumed that the transmitter has no knowledge about the channel of a passive eavesdropper.

3.2.3 Receiver Design

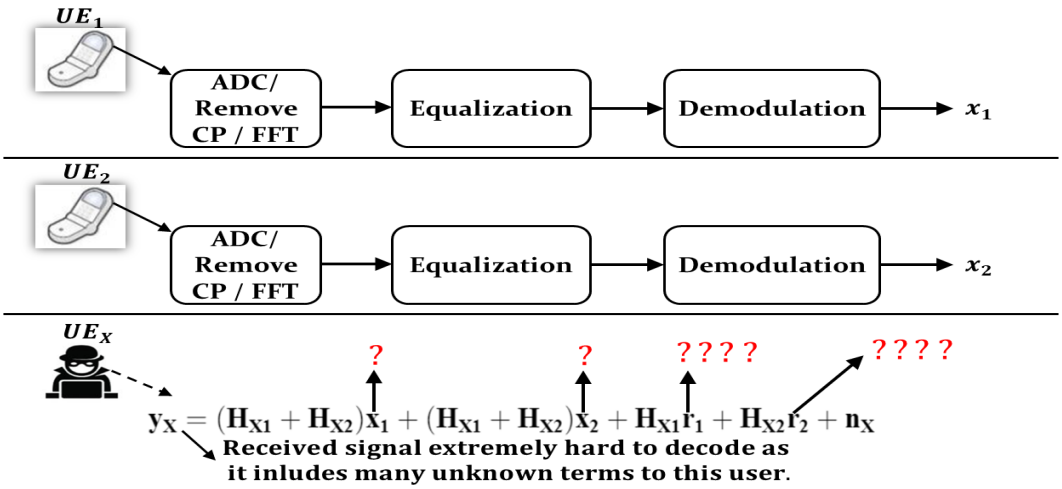

Figure 3.3: Receiver of MU-AS-ST.

MU-AS-ST has a simple receiver architecture where no additional computation is performed over conventional OFDM. The receiver of MU-AS-ST is presented in Fig.3.3, where the signal reception is shown at the legitimate nodes (UE_1 and UE_2) and the external eavesdropper equipment (UE_X). At each receiving end, the following operations are performed:

- *CP Removal & FFT*: The received samples are in time domain and as such first the added cycle prefixes are removed, then the FFT is taken to turn the samples to frequency domain.
- *Equalization*: After turning the received time samples to frequency domain, equalization by the effective channels is performed.
- *Symbol Demodulation*: After equalizing, the received samples are demodulated using conventional BPSK demodulation.

1) Received signal at the legitimate node UE_1

Let $\mathbf{y_{11}}$ and $\mathbf{y_{12}}$ stand for the received signals at the user equipment UE_1 through antennas $\boldsymbol{A_1}$ and $\boldsymbol{A_2}$, respectively. The received signal $\mathbf{y_1}$ is the sum of $\mathbf{y_{11}}$ and $\mathbf{y_{12}}$ as expressed by the following equations [1]:

$$\mathbf{y_1} = \mathbf{y_{11}} + \mathbf{y_{12}} + \mathbf{n_1} \tag{3.2}$$

$$\mathbf{y_1} = \mathbf{H_{11}}\mathbf{u_1} + \mathbf{H_{12}}\mathbf{u_2} + \mathbf{n_1} \tag{3.3}$$

$$\mathbf{y_1} = \mathbf{H_{11}}(\mathbf{x_1} + \mathbf{x_2} + \mathbf{r_1}) + \mathbf{H_{12}}(\mathbf{x_1} + \mathbf{x_2} + \mathbf{r_2}) + \mathbf{n_1} \tag{3.4}$$

$$\mathbf{y_1} = (\mathbf{H_{11}} + \mathbf{H_{12}})\mathbf{x_1} + (\mathbf{H_{11}} + \mathbf{H_{12}})\mathbf{x_2} + \mathbf{H_{11}}\mathbf{r_1} + \mathbf{H_{12}}\mathbf{r_2} + \mathbf{n_1} \tag{3.5}$$

2) Received signal at the legitimate node UE_2

Let $\mathbf{y_{21}}$ and $\mathbf{y_{22}}$ stand for the received signals at the user equipment UE_2 through antennas $\boldsymbol{A_1}$ and $\boldsymbol{A_2}$, respectively. The received signal $\mathbf{y_2}$ is the sum of $\mathbf{y_{21}}$ and $\mathbf{y_{22}}$ as expressed by the following equations:

$$\mathbf{y_2} = \mathbf{y_{21}} + \mathbf{y_{22}} + \mathbf{n_2} \tag{3.6}$$

$$\mathbf{y_2} = \mathbf{H_{21}}\mathbf{u_1} + \mathbf{H_{22}}\mathbf{u_2} + \mathbf{n_2} \tag{3.7}$$

$$\mathbf{y_2} = \mathbf{H_{21}}(\mathbf{x_1} + \mathbf{x_2} + \mathbf{r_1}) + \mathbf{H_{22}}(\mathbf{x_1} + \mathbf{x_2} + \mathbf{r_2}) + \mathbf{n_2} \tag{3.8}$$

$$\mathbf{y_2} = (\mathbf{H_{21}} + \mathbf{H_{22}})\mathbf{x_2} + (\mathbf{H_{21}} + \mathbf{H_{22}})\mathbf{x_1} + \mathbf{H_{21}}\mathbf{r_1} + \mathbf{H_{22}}\mathbf{r_2} + \mathbf{n_2} \tag{3.9}$$

3) Received signal at the external eavesdropping node UE_X

The external eavesdropper device receives the signals broadcasted by antennas $\boldsymbol{A_1}$ and $\boldsymbol{A_2}$. Let $\mathbf{y_{X1}}$ and $\mathbf{y_{X2}}$ stand for the received signals at the user equipment UE_2 through antennas $\boldsymbol{A_1}$ and $\boldsymbol{A_2}$, respectively. The received signal at the eavesdropping node can be expressed as:

$$\mathbf{y_X} = \mathbf{y_{X1}} + \mathbf{y_{X2}} + \mathbf{n_X} \tag{3.10}$$

$$\mathbf{y_X} = \mathbf{H_{X1}}\mathbf{u_1} + \mathbf{H_{X2}}\mathbf{u_2} + \mathbf{n_X} \tag{3.11}$$

$$\mathbf{y_X} = \mathbf{H_{X1}}(\mathbf{x_1} + \mathbf{x_2} + \mathbf{r_1}) + \mathbf{H_{X2}}(\mathbf{x_1} + \mathbf{x_2} + \mathbf{r_2}) + \mathbf{n_X} \tag{3.12}$$

$$\mathbf{y_X} = (\mathbf{H_{X1}} + \mathbf{H_{X2}})\mathbf{x_1} + (\mathbf{H_{X1}} + \mathbf{H_{X2}})\mathbf{x_2} + \mathbf{H_{X1}}\mathbf{r_1} + \mathbf{H_{X2}}\mathbf{r_2} + \mathbf{n_X} \tag{3.13}$$

[1] Note that the signals at all the receiving nodes are expressed in frequency domain (bold vectors as specified in the notation followed). These expressions hold right after the FFT process and this is for deriving the auxiliary signals in frequency domain so that they can be used at the transmitter of MU-AS-ST which is based on OFDM where the signal follows the following transitions:
Frequency Domain $\longmapsto$ Time Domain $\longmapsto$ Frequency Domain.

3.2.4 Design of the Auxiliary Signals

As highlighted in Figure 3.4, the received signal is a combination of a desired term, an interference term caused by other superimposed users and a term including the auxiliary signals which needs to be designed for cancelling the interference term totally. We may also interpret the interference term as a trial for internal eavesdropping. Thus, a successful design of the auxiliary signals is solving both the interference problem where every user experiences no interference at all from other superimposed users, and is provided with perfect secrecy against all kinds of eavesdropping activities from the part of the superimposed users (i.e., untrusted legitimate users). For an interference-

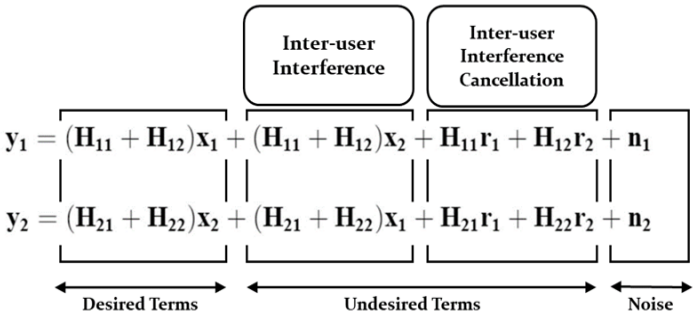

Figure 3.4: Desired and undesired terms in the received signal with respect to the superimposed users UE_1 and UE_2.

free and internally-secure communication, the conditions expressed by the following system $S_{(\mathbf{r_1},\mathbf{r_2})}$ need to be satisfied:

$$S_{(\mathbf{r_1},\mathbf{r_2})} \begin{cases} (\mathbf{H_{11}} + \mathbf{H_{12}})\mathbf{x_2} + \mathbf{H_{11}}\mathbf{r_1} + \mathbf{H_{12}}\mathbf{r_2} = 0 \\ (\mathbf{H_{21}} + \mathbf{H_{22}})\mathbf{x_1} + \mathbf{H_{21}}\mathbf{r_1} + \mathbf{H_{22}}\mathbf{r_2} = 0 \end{cases} \tag{3.14}$$

The solution of the system $S_{(\mathbf{r_1},\mathbf{r_2})}$ gives the following values for $\mathbf{r_1}$ and $\mathbf{r_2}$:

$$\mathcal{A} = \mathbf{H_{22}} - \mathbf{H_{21}}\mathbf{H_{11}^{-1}}\mathbf{H_{12}} \tag{3.15}$$

$$\nu = -(\mathbf{H_{21}} + \mathbf{H_{22}})\mathbf{x_1} + \mathbf{H_{21}}(\mathbf{I_{64}} + \mathbf{H_{11}^{-1}}\mathbf{H_{12}})\mathbf{x_2} \tag{3.16}$$

$$\mathbf{r_2} = \mathcal{A}^{-1}\nu \tag{3.17}$$

$$\mathbf{r_1} = (\mathbf{I_{64}} + \mathbf{H_{11}^{-1}}\mathbf{H_{12}})\mathbf{x_2} - (\mathbf{H_{11}^{-1}}\mathbf{H_{12}}\mathbf{r_2}) \tag{3.18}$$

For these values of the auxiliary signals [2], the inter-user interference is removed completely and internally-secure communication is established. The received signals at each user end is then given as follows:

$$\mathbf{y_1} = (\mathbf{H_{11}} + \mathbf{H_{12}})\mathbf{x_1} + \mathbf{n_1} \tag{3.19}$$

$$\mathbf{y_2} = (\mathbf{H_{21}} + \mathbf{H_{22}})\mathbf{x_2} + \mathbf{n_2} \tag{3.20}$$

$$\mathbf{y_X} = (\mathbf{H_{X1}} + \mathbf{H_{X2}})\mathbf{x_1} + (\mathbf{H_{X1}} + \mathbf{H_{X2}})\mathbf{x_2} + \mathbf{H_{X1}}\mathbf{r_1} + \mathbf{H_{X2}}\mathbf{r_2} + \mathbf{n_X} \tag{3.21}$$

[2] From this derivation it can be seen that $\mathbf{r_1}, \mathbf{r_2}$ will be a function of all the legitimate users' channels ($\mathbf{H_{11}}, \mathbf{H_{12}}, \mathbf{H_{21}}, \mathbf{H_{22}}$) and the legitimate users' data (i.e., $\mathbf{x_1}, \mathbf{x_2}$).

As shown from the equations above, the legitimate users can get their data by simple equalization while the illegitimate user (i.e., UE_X) receives a very distorted signal. This shows that the design of the auxiliary signals ensures perfect interference cancellation for the legitimate nodes while it creates a complex and extremely hard to decode signal at the external eavesdropping devices. Note that as the number of superimposed users grows, the complexity of this decoding grows as well.

3.3 Conventional PD-NOMA

In the conventional power domain NOMA setup, the base station (BS) transmits the same superimposed signal from both antennas simultaneously. The transmitted combined signal $\mathbf{q}$ can be written as:

$$\mathbf{q} = \sqrt{P}(\sqrt{\alpha_1}\mathbf{x_1} + \sqrt{\alpha_2}\mathbf{x_2}) \tag{3.22}$$

where P is the total transmit power. α_1 and α_2 denote the power allocation coefficients. In the rest of the analysis related to conventional power domain NOMA, we assume that UE_1 is the far user and UE_2 is the near user and thus $\alpha_1 > \alpha_2$.
Let $\mathbf{y_{1N}}, \mathbf{y_{2N}}$ and $\mathbf{y_{XN}}$ denote the signals received by UE_1, UE_2 and UE_X, respectively, using conventional power domain NOMA as the communication technique.
The received signal at the legitimate nodes and the external eavesdropper node can be written as follows:

$$\begin{bmatrix} \mathbf{y_{1N}} \\ \mathbf{y_{2N}} \\ \mathbf{y_{XN}} \end{bmatrix} = \begin{bmatrix} \mathbf{H_{11}} & \mathbf{H_{12}} \\ \mathbf{H_{21}} & \mathbf{H_{22}} \\ \mathbf{H_{X1}} & \mathbf{H_{X2}} \end{bmatrix} \begin{bmatrix} \mathbf{q} \\ \mathbf{q} \end{bmatrix} + \begin{bmatrix} \mathbf{n_1} \\ \mathbf{n_2} \\ \mathbf{n_X} \end{bmatrix} \tag{3.23}$$

which can be simplified as:

$$\begin{bmatrix} \mathbf{y_{1N}} \\ \mathbf{y_{2N}} \\ \mathbf{y_{XN}} \end{bmatrix} = \begin{bmatrix} \mathbf{H_{11}} + \mathbf{H_{12}} \\ \mathbf{H_{21}} + \mathbf{H_{22}} \\ \mathbf{H_{X1}} + \mathbf{H_{X2}} \end{bmatrix} \mathbf{q} + \begin{bmatrix} \mathbf{n_1} \\ \mathbf{n_2} \\ \mathbf{n_X} \end{bmatrix} \tag{3.24}$$

or,

$$\begin{bmatrix} \mathbf{y_{1N}} \\ \mathbf{y_{2N}} \\ \mathbf{y_{XN}} \end{bmatrix} = \begin{bmatrix} (\mathbf{H_{11}} + \mathbf{H_{12}})\mathbf{q} + \mathbf{n_1} \\ (\mathbf{H_{21}} + \mathbf{H_{22}})\mathbf{q} + \mathbf{n_2} \\ (\mathbf{H_{X1}} + \mathbf{H_{X2}})\mathbf{q} + \mathbf{n_X} \end{bmatrix} \tag{3.25}$$

Replacing $\mathbf{q}$ with its value expressed by (3.22), (3.25) becomes:

$$\begin{bmatrix} \mathbf{y_{1N}} \\ \mathbf{y_{2N}} \\ \mathbf{y_{XN}} \end{bmatrix} = \begin{bmatrix} (\mathbf{H_{11}} + \mathbf{H_{12}})\sqrt{P}(\sqrt{\alpha_1}\mathbf{x_1} + \sqrt{\alpha_2}\mathbf{x_2}) + \mathbf{n_1} \\ (\mathbf{H_{21}} + \mathbf{H_{22}})\sqrt{P}(\sqrt{\alpha_1}\mathbf{x_1} + \sqrt{\alpha_2}\mathbf{x_2}) + \mathbf{n_2} \\ (\mathbf{H_{X1}} + \mathbf{H_{X2}})\sqrt{P}(\sqrt{\alpha_1}\mathbf{x_1} + \sqrt{\alpha_2}\mathbf{x_2}) + \mathbf{n_X} \end{bmatrix} \tag{3.26}$$

Since UE_1 is the strong user (i.e., higher power share), this user equipment decodes its own signal $\mathbf{x_1}$ by treating the signal of the weak user, $\mathbf{x_2}$, as interference noise. The received signal at UE_1 can be written as:

$$\mathbf{y_{1N}} = (\mathbf{H_{11}} + \mathbf{H_{12}})\sqrt{P\alpha_1}\mathbf{x_1} + (\mathbf{H_{11}} + \mathbf{H_{12}})\sqrt{P\alpha_2}\mathbf{x_2} + \mathbf{n_1} \tag{3.27}$$

On the other hand, the user equipment UE_2 which is the near user receives the following signal:

$$\mathbf{y_{2N}} = (\mathbf{H_{21}} + \mathbf{H_{22}})\sqrt{P\alpha_1}\mathbf{x_1} + (\mathbf{H_{21}} + \mathbf{H_{22}})\sqrt{P\alpha_2}\mathbf{x_2} + \mathbf{n_2} \tag{3.28}$$

where the signal of UE_1 is dominating and thus, this user employs successive interference cancellation (SIC) to remove the effect of the signal of the far user. The received signal at UE_2 after the application of SIC can be written as follows:

$$\mathbf{y_{2N,SIC}} = (\mathbf{H_{21}} + \mathbf{H_{22}})\sqrt{P\alpha_2}\mathbf{x_2} + \mathbf{n_2} \tag{3.29}$$

Moreover, at the eavesdropper side the received signal can be expressed as:

$$\mathbf{y_{XN}} = (\mathbf{H_{X1}} + \mathbf{H_{X2}})\sqrt{P\alpha_1}\mathbf{x_1} + (\mathbf{H_{X1}} + \mathbf{H_{X2}})\sqrt{P\alpha_2}\mathbf{x_2} + \mathbf{n_X} \tag{3.30}$$

3.4 Performance Analysis

In this section, the performance analysis of MU-AS-ST is studied and compared to conventional PD-NOMA.

3.4.1 BER Analysis

Since BPSK is the modulation used in this design, the bit error rate of a legitimate user can be expressed as [32]:

$$BER_{UE_1,UE_2} = \frac{1}{2}\int_0^\infty erfc(\sqrt{\gamma_b})P_{\gamma_b}(\gamma_b), d\gamma_b \tag{3.31}$$

where $erfc(\cdot)$ is the complementary error function defined as $erfc(x) = \frac{2}{\sqrt{\pi}}\int_x^\infty \exp(-t^2)dt$. $P_{\gamma_b}(\gamma_b)$ stands for the probability distribution function (PDF) of the effective instantaneous signal to noise ratio of a legitimate user (i.e., UE_1, UE_2). $P_{\gamma_b}(\gamma_b)$ is related to the fading distribution through the following change of variable [30]:

$$P_{\gamma_b}(\gamma_b) = \frac{P_\alpha(\sqrt{\frac{\Omega\gamma_b}{\overline{\gamma_b}}})}{2\sqrt{\frac{\overline{\gamma_b}\gamma_b}{\Omega}}} \tag{3.32}$$

where $\alpha = \|\mathbf{H_{UE_i}}\|, i = 1, 2$ is the channel fading amplitude of a legitimate user. $\mathbf{H_{UE_i}} = \sum_{j=1}^{2}\mathbf{H_{ij}}$. Ω is defined as the mean square of the channel fading amplitude, i.e., $\Omega = \mathbb{E}[\alpha^2]$. $\overline{\gamma_b}$ denotes the average SNR.

Figure 3.5 shows the fading distribution of a legitimate user fitted with different known distribution functions. As shown, the effective channel can be fit with a Nakagami distribution with shape and scale parameters μ and ω. The fading distribution is characterized by the following system (S_α).

$$(S_\alpha)\begin{cases} P_\alpha(\alpha) = 2\left(\frac{\mu}{\omega}\right)^\mu \frac{1}{\Gamma(\mu)}\alpha^{2\mu-1}exp(-\frac{\mu}{\omega}\alpha^2) \\ (\mu,\omega) = (2.12853, 3.65843)\,. \end{cases} \tag{3.33}$$

where $\Gamma(.)$ is the gamma function.

After getting an expression for the fading amplitude, the PDF of the effective SNR expressed by Eq.(3.32) can be written as:

$$\begin{cases} P_{\gamma_b}(\gamma_b) = F\sqrt{\gamma_b}^{2(\mu-1)}exp(\frac{-\mu}{\omega}\frac{\Omega}{\overline{\gamma_b}}\gamma_b) \\ F = (\frac{\Omega}{\overline{\gamma_b}}\frac{\mu}{\omega})^\mu\frac{1}{\Gamma(\mu)}. \end{cases} \tag{3.34}$$

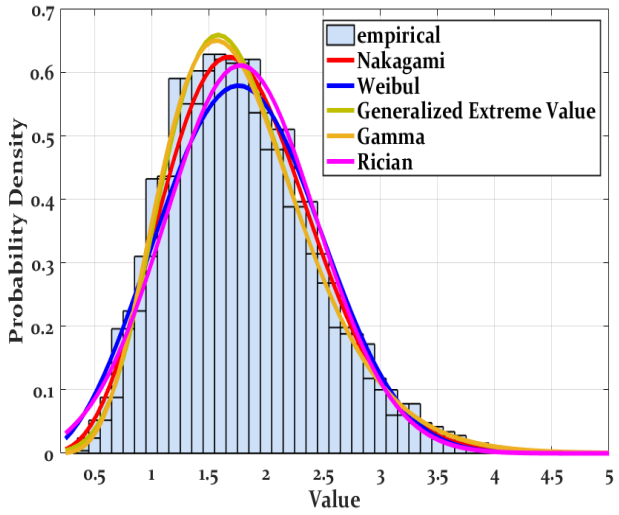

Figure 3.5: The amplitude distribution of the effective fading channel for the legitimate users UE_1 and UE_2.

By substituting (3.34) in the bit error rate equation of (3.31), the following integral is obtained:

$$BER_{UE_1,UE_2} = \frac{F}{2}\int_0^{\infty} erfc(\sqrt{\gamma_b})\sqrt{\gamma_b}^{2(\mu-1)} exp(\frac{-\mu}{\omega}\frac{\Omega}{\overline{\gamma_b}}\gamma_b), d\gamma_b \tag{3.35}$$

Moreover, the above integral is similar to a very known integration involving the complementary error function given in [31], as:

$$\int_0^{\infty} erfc(\sqrt{x})\sqrt{x}\exp(-\beta x)dx = \frac{1}{2\sqrt{\pi}}\left(\frac{arctan\left(\sqrt{\beta}\right)}{(\beta)^{3/2}} - \frac{1}{\beta(1+\beta)}\right), \beta > 0. \tag{3.36}$$

The bit error rate in (3.35) can be written in the form of this known integral by making $2(\mu-1) = 1$ which corresponds to setting $\mu = \frac{3}{2}$ instead of its original value, $\mu = 2.12853$. Note that it is feasible to perform this integration by taking $\beta = \frac{\mu}{\omega}\frac{\Omega}{\overline{\gamma_b}}$ which satisfies the condition $\beta > 0$.
Thus, the bit error rate of a legitimate user can be approximated by the following expression[3]:

$$\begin{cases} BER_{UE_1,UE_2} \approx \frac{F}{4\sqrt{\pi}}\left(\frac{arctan(\sqrt{\beta})}{(\beta)^{3/2}} - \frac{1}{\beta(1+\beta)}\right) \\ \beta = \frac{\mu}{\omega}\frac{\Omega}{\overline{\gamma_b}} \\ F = \frac{\beta^{\mu}}{\Gamma(\mu)} \\ (\mu,\omega) = \left(\frac{3}{2}, 3.65843\right) \end{cases} \tag{3.37}$$

where, $arctan\,(\cdot)$ is the inverse tangent function.

[3] A small note on this approximation is presented in Appendix C.

3.4.2 Secrecy Analysis

In this section, we discuss the security of the proposed design where we show that MU-AS-ST is robust against external and internal eavesdropping activities. External eavesdropping refers to the case of the external user equipment UE_X trying to decode the data of the legitimate superimposed users $\mathbf{x_1}, \mathbf{x_2}$. Internal eavesdropping refers to the case of the presence of an untrusted user among the superimposed users. We perform a comparative analysis with PD-NOMA.

3.4.3 Security Against Internal Eavesdropping

Unlike the data superposition principle in power domain NOMA where the far user signal receives the data of the near user (i.e., it is treated as noise during detection) and the near user employs SIC for subtracting the dominating far user's signal, in this design every legitimate user receives only its own signal where the interference from all other superimposed users in the network can be fully cancelled through the addition of the auxiliary signals. This presents a more robust design, compared to conventional NOMA, with no risk of internal eavesdropping activities in the presence of internal eavesdroppers among the superimposed users.

3.4.4 Security Against External Eavesdropping

From the receiver in Fig.3.6 and the derivation of the received signal at the eavesdropper node, UE_X, we can see that the decoding of the received signal is a very complex operation for the external eavesdropper node UE_X. This is due to the fact that the received signal at this node contains many unknowns including the legitimate users' data (i.e., $\mathbf{x_1}$, $\mathbf{x_2}$), their channels and the auxiliary signals $\mathbf{r_1}$ and $\mathbf{r_2}$. Moreover, the auxiliary signals, as can be seen from their derivation, are a complicated function of the user's channels and user's data signals which makes the decoding of the transmitted signals by an external device an extremely challenging task. Furthermore, the complexity of this decoding grows as the number of superimposed users grow.

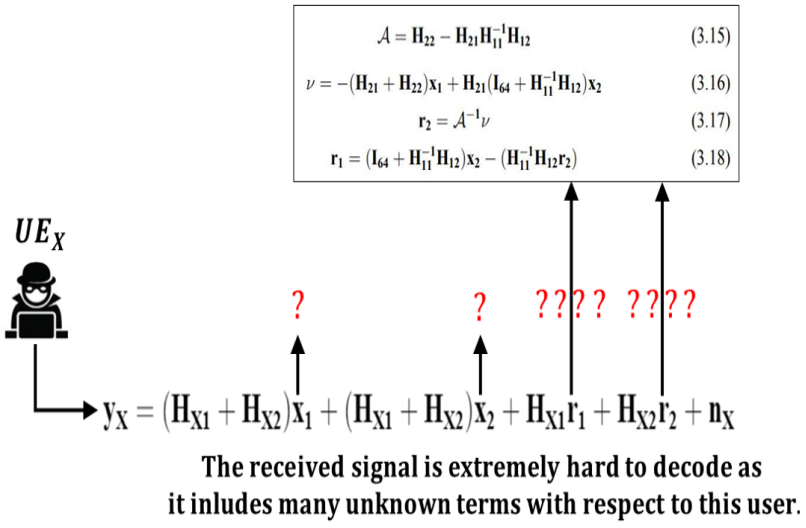

Figure 3.6: Received signal at the external eavesdropping device / MU-AST-ST

3.4.5 SINR Analysis: MU-AS-ST vs PD-NOMA

Legitimate Nodes ($\boldsymbol{UE_1}$,$\boldsymbol{UE_2}$)

In the following, we will derive the signal to interference plus noise ratio $(SINR)$ for the legitimate users using both the proposed MU-AS-ST and the conventional power domain NOMA. The $SINR$ metric for a given user equipment $\boldsymbol{UE} \in \{\boldsymbol{UE_1}, \boldsymbol{UE_2}, \boldsymbol{UE_X}\}$ using a technique $T \in \{MU-AS-ST, NOMA\}$ is defined as follows:

$$SINR^{T}_{\boldsymbol{UE}} = \frac{S}{I + \sigma_n^2} \tag{3.38}$$

where S,I and σ_n^2 stand, respectively,for the signal power, the interference power and the noise variance at the corresponding receiver node $\boldsymbol{UE}$.
From (3.19) and (3.20), $SINR$ for the legitimate users $\boldsymbol{UE_1}$ and $\boldsymbol{UE_2}$ using MU-AS-ST can be written as:

$$SINR^{MU-AS-ST}_{\boldsymbol{UE_1}} = \frac{\|\mathbf{H_{11}} + \mathbf{H_{12}}\|^2}{\sigma^2_{n_1}} \tag{3.39}$$

$$SINR^{MU-AS-ST}_{\boldsymbol{UE_2}} = \frac{\|\mathbf{H_{21}} + \mathbf{H_{22}}\|^2}{\sigma^2_{n_2}} \tag{3.40}$$

On the other hand, let's derive the $SINR$ for the legitimate users using conventional power domain NOMA.
First, for the far user, the received signal is shown by (3.27) and as can be seen from this equation it contains the interference from $\boldsymbol{UE_2}$ however since the far user's power share is the highest, this interference term is counted as noise and does not affect the detection of $\mathbf{x_1}$ by $\boldsymbol{UE_1}$. The corresponding $SINR$ for this user equipment can be written as:

$$SINR^{NOMA}_{\boldsymbol{UE_1}} = \frac{P\alpha_1\|\mathbf{H_{11}} + \mathbf{H_{12}}\|^2}{P\alpha_2\|\mathbf{H_{11}} + \mathbf{H_{12}}\|^2 + \sigma^2_{n_1}} \tag{3.41}$$

Moreover, since the near user removes the interference caused by the far user, the $SINR$ for this user for decoding its own signal $\mathbf{x_2}$ can be derived from (3.29) as:

$$SINR^{NOMA}_{\boldsymbol{UE_2}} = \frac{P\alpha_2\|\mathbf{H_{21}} + \mathbf{H_{22}}\|^2}{\sigma^2_{n_2}} \tag{3.42}$$

3.4.6 Computational & Design Complexity Analysis

In conventional NOMA, the main operation is successive interference cancellation where near users performs SIC for the far users' signals and then decode their own signals. This is regarded as one of the main sources of complexity in the NOMA receiver and thus it introduces a delay in the communication.
Unlike SIC, this design cancels the interference completely, with no risks of internal eavesdropping as in the case of NOMA. Moreover, the use of diagonal of matrices, in the proposed design, keeps the computational cost very minimal at the transmitter freeing the receiver from any complex processing. Furthermore, performing all the processing at the transmitter makes the proposed paradigm a very appealing choice for internet of things (IoT) applications.

3.5 Simulation Results

Table 3.2: MU-AS-ST / Simulation Parameters

Parameter	**Value**
Modulation type	BPSK
IFFT / FFT size	64
Subcarriers for data n	52
Symbols allocated for cyclic prefix	16
Number of inactive sub-carriers for out of band emission	12
Number of OFDM symbols	2×10^4
Channel model	Rayleigh
Multipath channel delay samples locations	[0 3 5 6 8]
Multipath channel tap power profile (dBm)	[0 -8 -17 -21 -25]

Computer simulations of the proposed MU-AS-ST were performed using the MATLAB simulation environment. The performance is measured in terms of metrics such as the bit error rate, throughput and PAPR. The list of all the parameters used in the simulations are shown in Table 3.2.

3.5.1 BER

In Figure 3.7, the bit error rate simulation results of MU-AS-ST are displayed. We

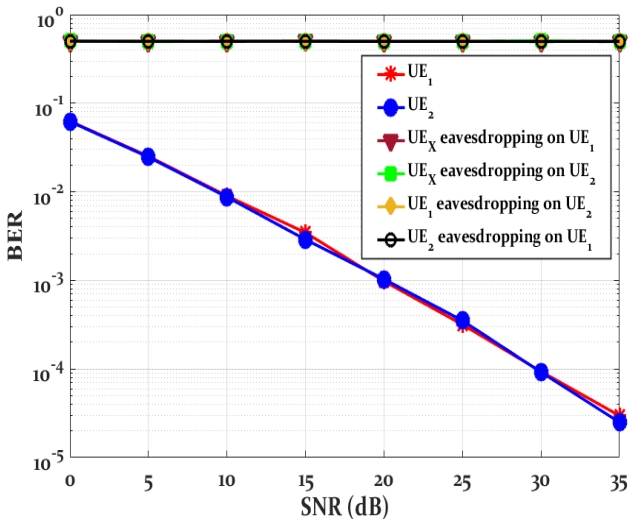

Figure 3.7: Bit error rates; where legitimate users have a good performance while all internal and external eavesdroppers have severe BER degradation.

can see that the legitimate users get a very satisfactory BER performance while in all eavesdropping activities a very poor performance is recorded. This includes: 1) internal eavesdropping trials which correspond to the presence of an untrusted user among the superimposed users. 2) external eavesdropping where an illegitimate user

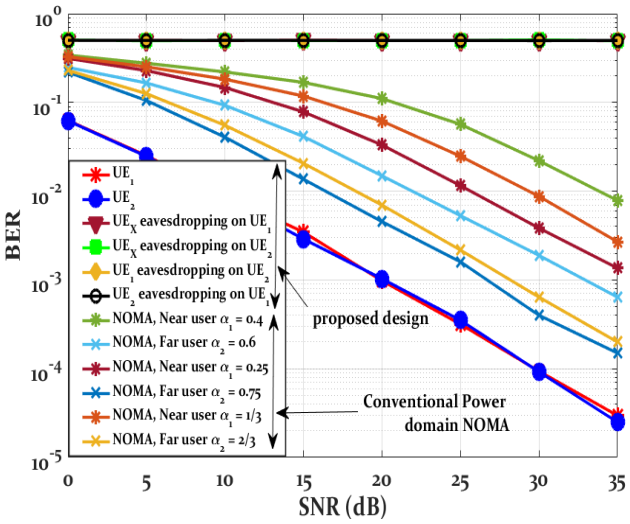

Figure 3.8: Bit error rate of MU-AS-ST compared to conventional power domain NOMA under various power allocation scenarios.

(i.e., not among the superimposed users) tries to decode the broadcasted data. In Figure 3.8, MU-AS-ST is compared to power domain NOMA under various power allocation scenarios. It can be observed that MU-AS-ST surpasses power domain NOMA in all the considered cases.

3.5.2 Throughput

Throughput is an important metric for evaluating the performance of any communication system; however it is specifically important as a metric in the assessment of multiple access designs.
Throughput simulations of the proposed design are presented in Figure 3.9 where it is shown that the legitimate nodes achieve good spectral gain while all eavesdropping scenarios exhibit a degradation in their performance. The total throughput saturates at 2 since the design developed here superimposes two users.

3.5.3 PAPR

Since MU-AS-ST employs conventional OFDM as its basis waveform, the PAPR simulations of MU-AS-ST were performed and it was shown that MU-AS-ST does not add further degradation over conventional OFDM in terms of PAPR, it even achieves slightly lower values at high values on the x-axis as shown in Fig.3.10.

3.6 Conclusion

In this chapter, the design termed as Multi-User Auxiliary Signal Superposition Transmission (MU-AS-ST) have been proposed and studied. The performance of the proposed design in addressing the shortcomings of current conventional power domain

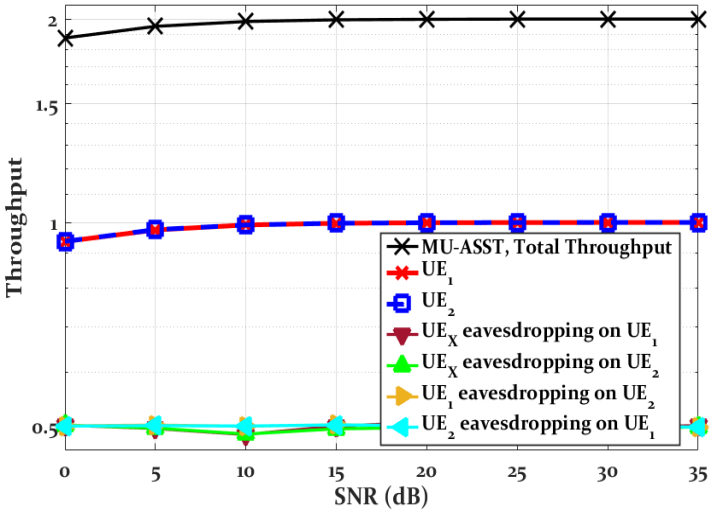

Figure 3.9: Throughput of the legitimate/eavesdropper nodes in the network, using the proposed MU-AS-ST.

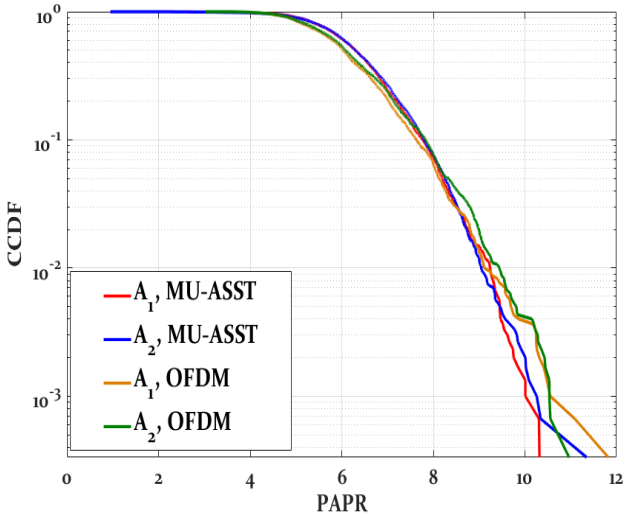

Figure 3.10: PAPR of MU-AS-ST compared to conventional OFDM.

NOMA have been evaluated and simulated in a Rayleigh fading channel through mathematical derivations and computer simulations.
The proposed design, which is based on the auxiliary signals, was shown to be less-complex compared to conventional PD-NOMA where successive interference is linked with increased design complexity and risks of internal eavesdropping in the presence of an untrusted user among the superimposed users. Moreover, the use of diagonal matrices in the proposed design makes the computational processing easier. This is with all the processing being done at the transmitter thus freeing the receiver from any additional computation over a conventional OFDM receiver.
MU-AS-ST is secure against both internal and external eavesdropping activities where each legitimate user receives its own data with no interference from other superimposed users. Moreover, the external passive eavesdropper receives a signal which is

very hard to decode since it contains a lot of unknowns with respect to this device which makes the decoding extremely challenging for this illegitimate node. The order of complexity in decoding this data by an illegitimate device grows as more number of users are superimposed; however it is even a challenging task in the case of two superimposed users which was studied in this thesis.
In terms of PAPR, MU-AS-ST was shown to add no further degradation to the conventional OFDM PAPR where it even reduces it slightly at high SNR values.

Chapter 4

Enhancing the Spectral Efficiency per Area and per Device through Multi-Access Multi-dimensional OFDM Modulations

4.1 Introduction

The exploration of the subcarriers' power inside an OFDM block was studied in chapter 2 and was shown to lead to doubling the spectral efficiency per device. Moreover, MU-AS-ST was presented in chapter 3 as a multiple access alternative for the conventional power domain NOMA.
In this chapter, we present another design which explores the integration of multi-dimensional OFDM modulation formats with multiple access designs by studying the examplary integration of OFDM-SPM-BPSK [1] and MU-AS-ST. This combination of multi-dimensional OFDM modulation formats and multiple access techniques leads to the enhancement of both of the spectral efficiency categories discussed in chapter 2, where the spectral efficiency per area is enhanced through the use of the multiple access setup (i.e., many devices/users in the same geographical area are supported by the same limited resources simultaneously) and the spectral efficiency per receiving device is increased through the use of multi-dimensional OFDM modulations formats by embedding more data bits in the transmitted stream through the exploration of additional dimensions in the OFDM waveform such as the subcarriers' index/power/number..etc as shown in the illustrative plot Fig.4.1. This integration is a promising solution for a better usage of the spectrum allocated for wireless communications.
Particularly, we have seen that if the power of the subcarriers is explored as a dimension then, the spectral efficiency per device is doubled due to the exploration of every subcarrier in the OFDM block unlike other dimensions (index, number, ..etc) where only the active subcarriers convey data implying only a partial enhancement of the data rate.
In summary, the integration of OFDM-SPM-BPSK and MU-AS-ST achieves the following contribution points:

[1] Note that this design is fully coherent. OFDM-SPM-BPSK is the coherent version of the design proposed in chapter 2. For more on this design, the reader is directed to publication 4, in section D.

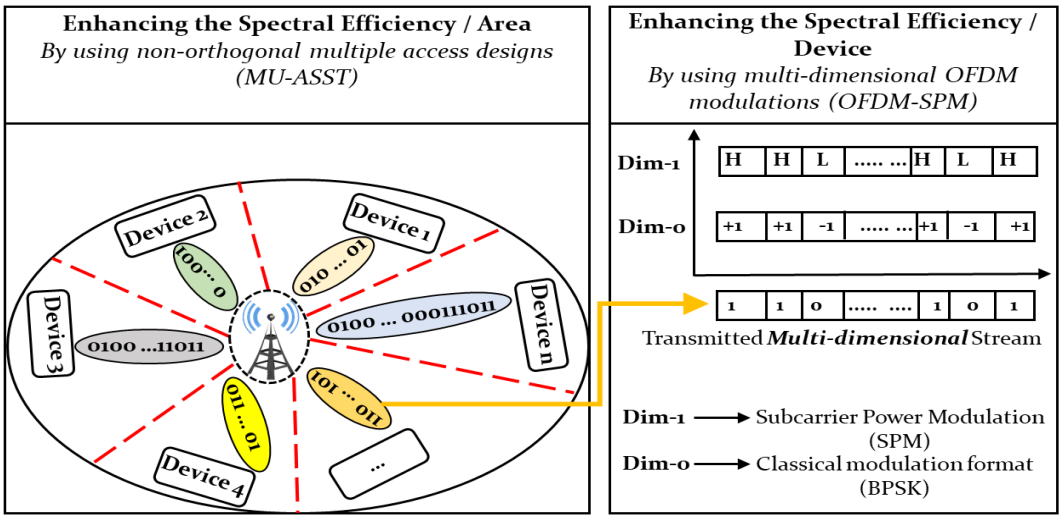

Figure 4.1: Enhancing the spectral efficiency per area and per device by integrating multi-dimensional OFDM modulations with multiple access schemes.

- Doubling the spectral efficiency per area through the use of MU-AS-ST, where two users in the same area are simultaneously supported with the same set of resources.
- Doubling the spectral efficiency at each user node due to the exploration of the power as an additional dimension.

The proposed design in this chapter is termed as D-SEAD (Doubling the Spectral Efficiency per Area and per Device).

4.2 Proposed System Model

4.2.1 Transmitter Design

The transmitter of the proposed design is shown in Fig.4.2 where the incoming data streams of UE_1 and UE_2 are first modulated using OFDM with Subcarrier Power Modulation and Binary Phase Shift Keying (OFDM-SPM-BPSK). This corresponds to

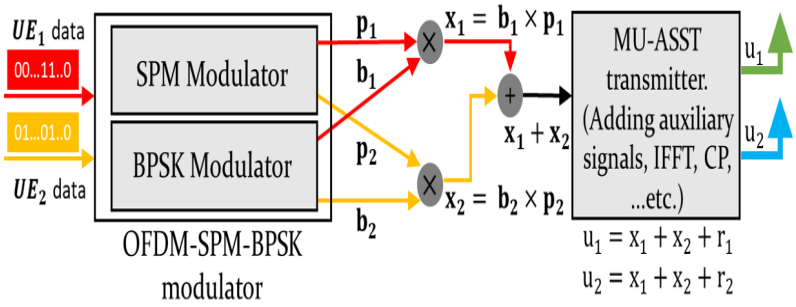

Figure 4.2: Transmitter of the proposed design.

modulating the incoming bit-stream for each user user independently using the classical BPSK modulation and through the subcarrier power modulation where the incoming bits are converted to high and low levels H, L, as explained in detail in the transmitter of NC-OFDM-SPM presented in chapter 2. After the independent modulations through BPSK (i.e., $\mathbf{b_1}, \mathbf{b_2}$) and the power subcarrier modulation block (i.e., $\mathbf{p_1}, \mathbf{p_2}$), the joint data streams (i.e., $\mathbf{x_1} = \mathbf{b_1} \times \mathbf{p_1}, \mathbf{x_2} = \mathbf{b_2} \times \mathbf{p_2}$) for both users are superimposed (i.e., $\mathbf{x_1} + \mathbf{x_2}$). The auxiliary signals $\mathbf{r_1}, \mathbf{r_2}$ are added on top of the superimposed data and two signals $u_1 = x_1 + x_2 + r_1$ and $u_2 = x_1 + x_2 + r_2$ are transmitted from two different antennas A_1 and A_2, respectively.

4.2.2 Receiver Design

The same setup used in the study of MU-AS-ST is used here where a network composed of three nodes of which two are legitimate users (i.e., UE_1, UE_2) and an external eavesdropping device UE_X. Moreover, the receiver of this design is not much different than the receiver of the MU-AS-ST scheme presented in chapter 3. The only difference lies at the demodulation stage, where in this design two separate demodulation blocks are used as shown in the receiver diagram in Fig.4.3:

- *BPSK Demodulator:* demodulates the incoming combined stream using conventional BPSK demodulation. The output of this block is the BPSK bit stream.
- *SPM Demodulator:* This demodulator is for the detecting the bits conveyed through the exploration of the power of the subcarriers inside the OFDM block. This is the same demodulator as in the receiver of NC-OFDM-SPM treated in chapter 2. This demodulator compares the power of the incoming symbols to a predefined threshold defined as in Eq.(2.2) and the recovers the high (H) and low (L) power bits.

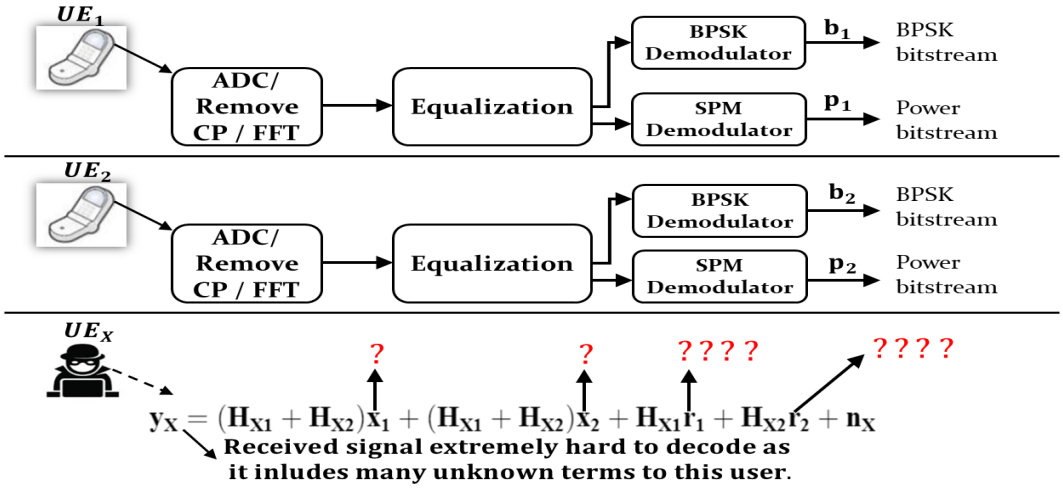

Figure 4.3: Receiver of the proposed design.

4.3 Results & Discussion

4.3.1 BER Analysis

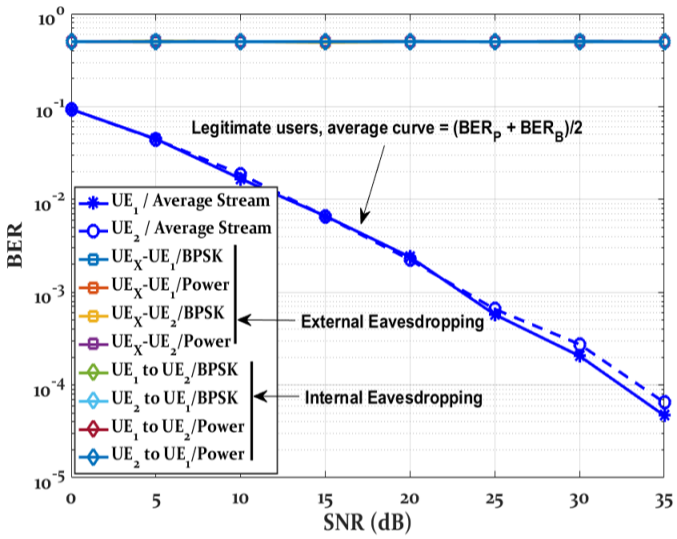

Figure 4.4: Bit error rate of MU-AS-ST with OFDM-SPM-BPSK, under the optimized power reassignment (PRP-OOP).

Simulations of the design proposed in this chapter were done using the same simulation parameters used in chapter 2 and 3. Furthermore, OFDM-SPM-BPSK is used as the modulation technique in the optimized power reassignment mode (or Overall Optimized Performance (OOP)) where the power levels are $(H, L) = (1, 918, 0.5668)$. In Fig.4.4, the average bit error rates for the legitimate users are plotted along with the error rates which simulate all the eavesdropping scenarios. It can be seen that the average curve attains the same BER performance as in the case of MU-AS-ST without the subcarrier power modulation. By looking at Fig.4.5, where the individual curves

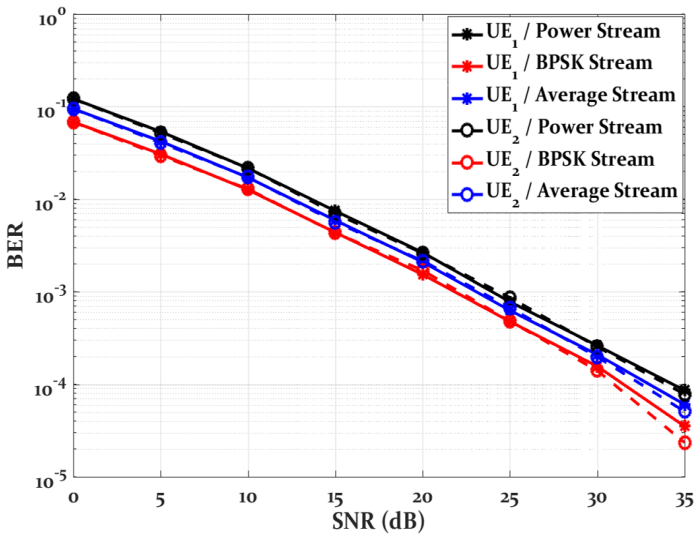

Figure 4.5: Bit error rates for the legitimate users UE_1, UE_2.

corresponding to the detection of the BPSK bits and the detection of the power bits are displayed, it is observed that the BPSK stream attains a lower error rate compared to the average curve which also represents the plain MU-AS-ST case. This is due to the reassignment mechanism which enhanced the overall reliability of the system making it better than the case of MU-AS-ST without OFDM-SPM-BPSK integrated with it. Moreover, the power curve for a legitimate user is slightly worse than performance of the conventional MU-AS-ST presented in chapter 3.
Furthermore, it can be seen from Fig.4.4 that in all eavesdropping scenarios, there is extremely severe degradation in the performance showing the secrecy of the proposed scheme. The degraded curves represent:

- *External eavesdropping cases:* This corresponds to the case where the external illegitimate device UE_X tries to decode the data of the legitimate users UE_1 and UE_2. It is shown that decoding any stream (the power or BPSK) is not feasible due to the secure design through the auxiliary signals.

- *Internal eavesdropping cases:* This simulates the case of untrusted users among the superimposed users. As shown in chapter 3, MU-AS-ST is secure against internal eavesdropping trials as well and as such decoding the power or the BPSK streams is not feasible as shown in Fig.4.4.

4.3.2 Spectral Efficiency

In Fig.4.6, the data rates of the legitimate users are displayed. The following results can be concluded from this plot:

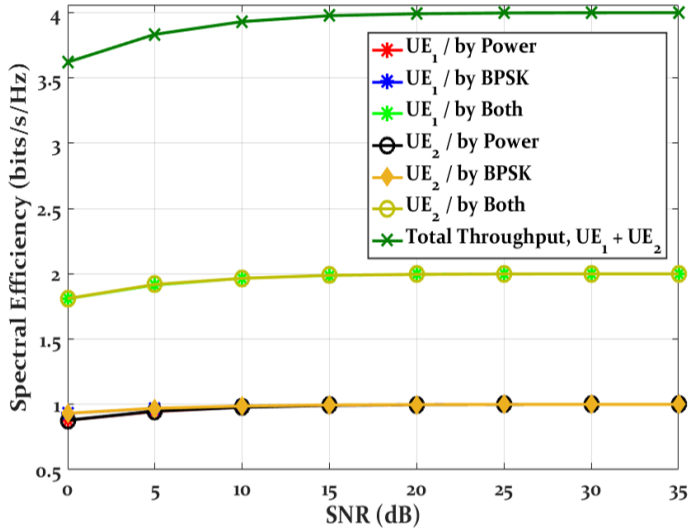

Figure 4.6: Spectral efficiency of MU-AS-ST using OFDM-SPM-BPSK as the modulation technique.

- *Doubling the spectral efficiency per device:* It can be seen that the spectral efficiency per user/device is doubled for each one of legitimate users UE_1 and UE_2. This is due to the use of OFDM-SPM-BPSK which is a 2-D modulation format as discussed in chapter 2. This leads to doubling the spectral efficiency since

data is sent through the BPSK constellation and through the subcarrier power levels.

- *Doubling the spectral efficiency per area:* The overall spectral efficiency of the system or the overall achievable rate can be found by summing the rates of the individual users in the network and as can be seen from the spectral efficiency plot, the overall data rate (for two users $UE_1 + UE_2$) is doubled amounting to 4 bits/s/Hz.

4.3.3 PAPR

Since this design is based on OFDM, it is important to evaluate its performance in terms of peak to average power ratio and check if it adds any additional degradation over conventional OFDM. In Fig.4.7, results of the PAPR simulations for two transmit signals from two different antennas A_1 and A_2 are displayed where it can be observed that the proposed design attains almost the same PAPR as conventional OFDM with DPSK and it does not add any further degradation over it. Furthermore, PAPR reduction techniques can be implemented with this setup to enhance the performance.

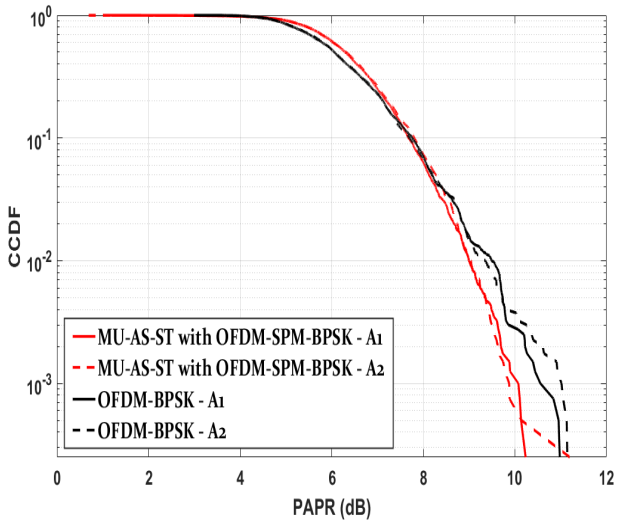

Figure 4.7: PAPR of MU-AS-ST using OFDM-SPM-BPSK as the modulation technique.

4.3.4 Complexity Analysis

This design adds very slight complexity to the system proposed in chapter 3. The only additional processing units over conventional MU-AS-ST are the SPM modulator at the transmitter and the SPM demodulator at the receiver. Note that since SPM employs threshold based detection this adds slight complexity over the conventional BPSK demodulator unlike ML-detector and LLR detector based multi-dimensional OFDM modulations such as index modulations [20].

4.4 Conclusion

In this chapter, OFDM-SPM-BPSK was used as the modulation option for the multiple access design MU-AS-ST developed in chapter 3. Results have shown that this combination reaches doubling the spectral efficiency per area through the use of MU-AS-ST and the spectral efficiency per device through the use of OFDM-SPM-BPSK which doubles the spectral efficiency per receiving node as it explores the power of the OFDM subcarriers as an additional dimension to send an additional (second) data stream along with the classical BPSK stream.

Appendix A

Constellation diagram: NC-OFDM-SPM vs 4-PAM

[1] The constellation diagram of Fig.A.1 reveals a close similarity between the proposed NC-OFDM-SPM and Pulse Amplitude Modulation (PAM). To further clarify this ambiguity raised by the similarity of both constellations, we consider Fig.A.1 for highlighting the structural difference that exists between both schemes. First, as explained in the system model of OFDM-

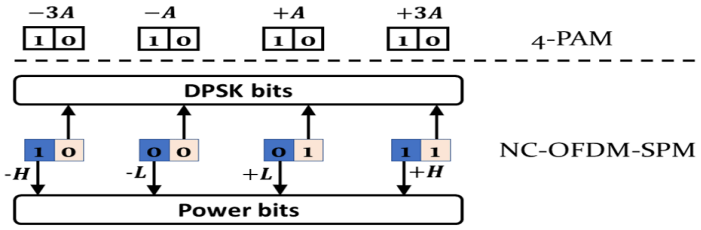

Figure A.1: Comparison between the constellation diagram of OFDM-SPM and 4-PAM.

SPM and shown in the simulation results, the OFDM-SPM waveform results from the combination of two main operations: conventional OFDM with DPSK modulation and Subcarrier Power Modulation (SPM) which corresponds to manipulating the power level of the transmit subcarriers by setting it to high (H) or low (L). The power allocator block in the transmitter diagram of NC-OFDM-SPM is the unit responsible for this latter operation. In other words, the power of the subcarriers is used as an extra dimension for conveying extra data bits.
Moreover, as shown in Fig.A.1, even though any pair of bits *"ij"* appears to be in the same position of the constellation diagram of both NC-OFDM-SPM and 4-PAM, this pair is a result of different operations in both cases. That's, in the case of OFDM-SPM, the pair *"ij"* corresponds to a power subcarrier (i.e, low if $'i' = 0$ and high if $'i' = 1$) carrying a bit $'j'$ modulated by DPSK. On the other hand, in the upper subplot where PAM is represented all the pairs are colored with the same color showing the fact that they are all resulting from classical 4-PAM modulation and, unlike OFDM-SPM, no extra dimension is explored to convey extra data bits. Furthermore, exploring the subcarriers' power is the same principle employed in index modulation (OFDM-IM) where the positions (indices) of the active subcarriers can be selected according to a look-up table for conveying extra data bits. In fact, the difference between OFDM-SPM and PAM is the same as the difference between OFDM-IM and pulse position modulation (PPM).

[1] Some of the appendices given here are replies to comments from the reviewers during the publication of the papers related to this project. Some are mere explanations to clarify the text or discussions of future research ideas related to the proposed designs.

Appendix B

Error floor problem: A discussion on the logic of combining subcarrier power modulation & differential detection.

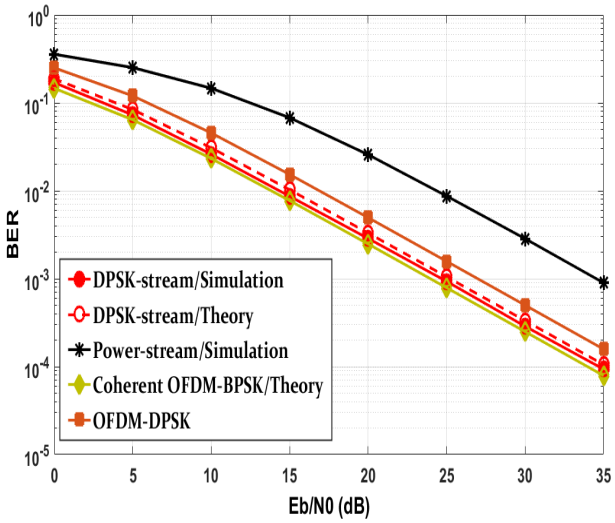

Figure B.1: Bit error rates for NC-OFDM-SPM in the PRP-ACP mode.

During the submission of publication 1, where the proposed non-coherent design was shown to achieve the performance of coherent OFDM-BPSK, one of the reviewers commented, among other comments, with the following:
Comment: *While encoding information over positive amplitudes looks quite straightforward, reliable communication in non-coherent systems based on amplitude modulation can be a bit tricky ;). To see this I would kindly suggest the authors to first forget about combining amplitude modulation with differential scheme and only develop a two-level power modulation with positive levels A>a>0. You will immediately come to this conclusion that even under optimal ML receiver the performance of non-coherent communication is not satisfactory. More specifically, such a system shows an error floor for any fixed value of A>0 and a>0. This error-floor cannot be seen in Fig. 3 and there should be some satisfactory explanations in this regard.*

I would like to comment on this claim as follows [1]:

1. Right. there should be an error floor which is, by the way, clear from Fig/2.14[2] where

[1] This comment is included here because it is one of the interesting comments (or the most interesting) i had during the publication of papers related to design 1. Moreover, it needs a reply since it poses problems directly related to the feasibility of the idea.

[2] Fig.2.14 is displayed here again for easier reading.

the power stream achieves higher BER than the DPSK stream.

2. Unlike classical modulations (PAM alone , or DPSK alone, ..etc), there is a flexibility with multi-dimensional OFDM modulations. This means that, for reaching a wanted performance for a specific user some optimization problem can be defined by putting constraints on the individual curves. In our case for example, the power stream was scarified for the DPSK stream for this latter to reach the performance of coherent OFDM-BPSK, as shown in the PRP-ACP mode. Reaching the coherent performance with the DPSK curve introduced some degradation in the power curve as can be seen from Fig.2.14; however, this power stream is an additional benefit given by NC-OFDM-SPM where it can be reallocated for a user application where ultra-reliability is not a main requirement.

Appendix C

A note on the derivation of the BER expression of MU-AS-ST

We have seen that the BER of a legitimate user, using MU-AS-ST, can be approximated by Eq.3.37 as follows:

$$\begin{cases} BER_{UE_1,UE_2} \approx \frac{F}{4\sqrt{\pi}} \left(\frac{arctan(\sqrt{\beta})}{(\beta)^{3/2}} - \frac{1}{\beta(1+\beta)} \right) \\ \beta = \frac{\mu}{\omega} \frac{\Omega}{\overline{\gamma_b}} \\ F = \frac{\beta^{\mu}}{\Gamma(\mu)} \\ (\mu, \omega) = \left(\frac{3}{2}, 3.65843\right) \end{cases} \tag{C.1}$$

Note that this is only an approximate expression for the BER and is not very accurate due to the change of the scale parameter μ (the original distribution is modified as shown in Fig.C.1 for the purpose of converting the BER integral into a solvable one). The exact performance can be obtained from the simulation curves. This theoretical expression is only given as an additional result over the simulation curves where one can obtain an approximate value of the BER performance of MU-AS-ST at any SNR.

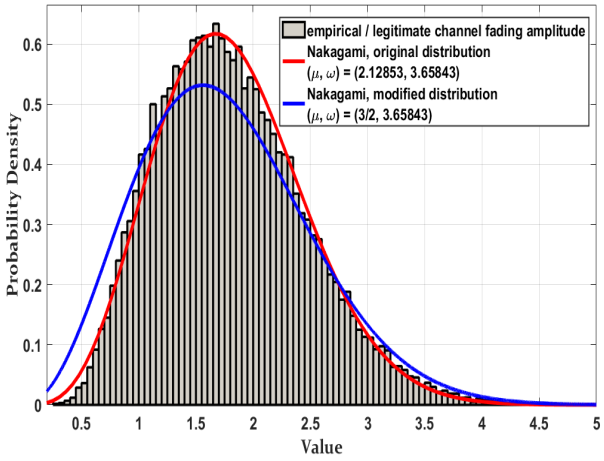

Figure C.1: The amplitude distribution of the effective fading channel for the legitimate users UE_1 and UE_2. Original and modified distributions.

Appendix D

A short discussion on security

In chapter 2, NC-OFDM-SPM was studied in terms of addressing the requirements of future wireless systems such as reliability, spectral efficiency, complexity and latency, PAPR; however, a study on the security of this design was not performed.
One possible way for achieving the security of this waveform is through chaotic communication techniques where a chaotic map can be designed for this purpose. Examples of possible maps are chaotic symbolic dynamics and others. Particularly, for reducing the complexity and the problems of synchronization, non-coherent chaotic setups, rather than coherent maps, can be explored for this purpose. A system model for the security of OFDM-SPM through chaotic

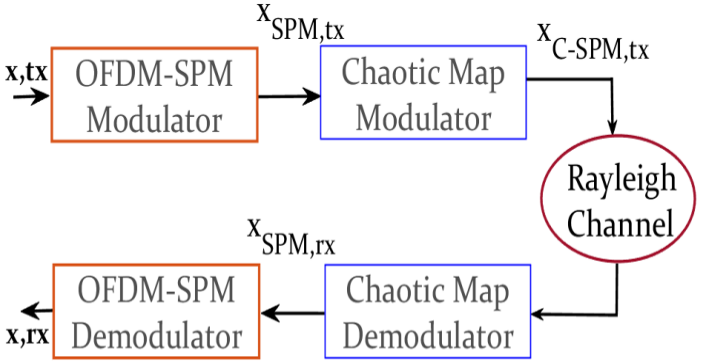

Figure D.1: System model for securing OFDM-SPM through chaotic maps.

maps is presented in the figure below where after the joint stream is formed it can be given as an input to a chaotic system which changes its settings in each transmission and outputs a chaotic sequence in each step due its sensitivity to initial conditions.

Moreover, In chapter 4, the integration of subcarrier power modulation and MU-AS-ST was studied where a secure transmission method which doubles the spectral efficiency per area and per device was developed and the security was achieved through specifically designed auxiliary signals. Although, the achieved security is enough as shown by the results; the idea presented above can be used for designing an extra robust and solid security mechanism, on top of the auxiliary signals, through the use of chaotic maps as shown in the figure above. In this way, the eavesdropper is more challenged by facing three levels of difficulty as shown in Fig.D.2:

- *Chaotic map level.* There is an extremely low probability of mapping the received chaotic sequence to the original transmitted data (i.e., input to the chaotic modulator). This is the first level to be passed by the eavesdropper and it is extremely hard since it is related to a chaotic behavior which changes in every round.

- *Multiple access / auxiliary signals level.* The second level to be passed by the eavesdropper is the knowledge of the auxiliary signals which was shown, from the design of MU-AS-ST, to be extremely challenging for the eavesdropper device as it is the combination of the users' data x_1, x_2, the users' channels, and the auxiliary signals r_1, r_2 which are all unknowns to this device.
- *the multi-dimensional modulation level.* After decoding the superimposed data x_1, x_2 the eavesdropper needs to decode from it the individual power (i.e., p_1, p_2) and BPSK streams (i.e., b_1, b_2). This is not hard compared to the previous two levels; however, reaching it is challenging due to the difficulty of the steps that come before it.

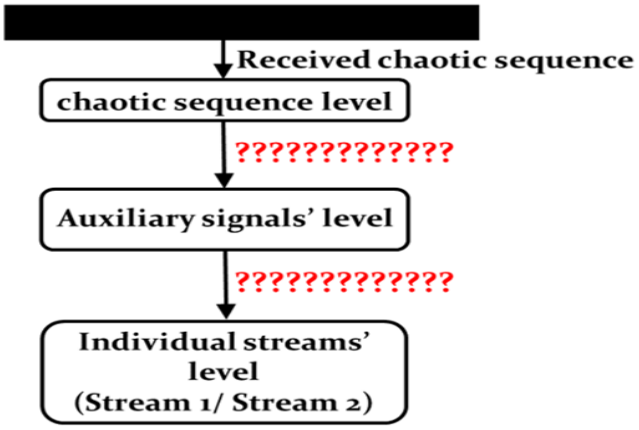

Figure D.2: Different layers of security / through auxiliary signals and through chaotic maps.

Bibliography

[1] M. Agiwal, A. Roy, and N. Saxena, "Next generation 5G wireless networks: A comprehensive survey,"IEEE Communications Surveys Tutorials, vol. 18, no. 3, pp. 1617–1655, third quarter 2016.

[2] L. Dai, B. Wang, Z. Ding, Z. Wang, S. Chen, and L. Hanzo, "A survey of non-orthogonal multiple access for 5G,"IEEE Communications Surveys Tutorials, vol. 20, no. 3, pp. 2294–2323, third quarter 2018.

[3] Y. Liu, Z. Qin, M. Elkashlan, Y. Gao, and A. Nallanathan, "Non-orthogonal multiple access in massive MIMO aided heterogeneous networks," in2016 IEEE Global Communications Conference (GLOBECOM), Dec 2016, pp. 1–6.

[4] A. Sabharwal, P. Schniter, D. Guo, D. W. Bliss, S. Rangarajan, and R. Wichman, "In-band full-duplex wireless: Challengesand opportunities,"IEEE Journal on Selected Areas in Communications, vol. 32, no. 9, pp. 1637–1652, Sep. 2014.

[5] R. Mesleh, H. Haas, C. W. Ahn, and S. Yun, "Spatial modulation – OFDM," 02 2019.

[6] R. Abu-alhiga and H. Haas, "Subcarrier-index modulation OFDM," in 2009 IEEE 20th International Symposium on Personal, Indoor and Mobile Radio Communications, Sep. 2009, pp. 177–181.

[7] E. Basar, Ümit Aygölü öu, E. Panayirci, and H. V. Poor, "Orthogonal frequency division multiplexing with index modulation,"2012 IEEE Global Communications Conference (GLOBECOM), pp. 4741–4746, 2012.

[8] A. M. Jaradat, J. M. Hamamreh, and H. Arslan, "OFDM with subcarrier number modulation,"IEEE Wireless Communications Letters, vol. 7, no. 6, pp. 914–917, Dec 2018.

[9] Jaradat, Ahmad & Hamamreh, Jehad. (2020). Orthogonal Frequency Division Multiplexing With Subcarrier Gap Modulation. 10.1109/PIMRC48278.2020.9217187.

[10] A. Jaradat, J. Hamamreh, and H. Arslan, "Modulation options for OFDM-based waveforms: Classification, comparison,and future directions,"IEEE Access, vol. 7, pp. 17 263–17 278, 2019.

[11] A. Hajar, J. M. Hamamreh, M. Abewa, and Y. Belallou, "A spectrally efficient OFDM-based modulation scheme for future wireless systems," in2019 Scientific Meeting on Electrical-Electronics Biomedical Engineering and Computer Science(EBBT), April 2019, pp. 1–4.

[12] Hamamreh, JM, Hajar, A, Abewa, M. Orthogonal frequency division multiplexing with subcarrier power modulation for doubling the spectral efficiency of 6G and beyond networks. Trans Emerging Tel Tech. 2020; 31:e3921. https://doi.org/10.1002/ett.3921

[13] Xu, Chao , Ishikawa, Naoki , Rajashekar Rakshith , Sugiura Shinya , Maunder Robert , Wang Zhaocheng , Yang Lie-Liang , Hanzo, L.. (2019). Sixty Years of Coherent Versus Non-coherent Trade-offs and the Road from 5G to Wireless Futures. IEEE Access. 10.1109/ACCESS.2019.2957706.

[14] P. Jung and P. Walk, "Sparse Model Uncertainties in Compressed Sensing with Application to Convolutions and Sporadic Communication", in Compressed Sensing and its Applications: MATHEON Workshop 2013, H. Boche, R. Calderbank, G. Kutyniok, and J. Vybiral, Eds., Springer, 2015.

[15] Fernando N, Hong Y,Viterbo E. Self-Heterodyne OFDM Transmission for Frequency Selective Channels. IEEE Transactions on Communications 2013; 61(5): 1936-1946. doi: 10.1109/TCOMM.2013.021913.120510

[16] Fernando, T. N. C., Emanuele, V., Monash University, Monash University. (2014). Non-coherent OFDM techniques.

[17] Jin Q, Hong Y. Self-Coherent OFDM With Undersampling Downconversion for Wireless Communications. IEEE Transactions on Wireless Communications 2016; 15(10): 6979-6991. doi: 10.1109/TWC.2016.2594176

[18] Choi J. Noncoherent OFDM-IM and Its Performance Analysis. IEEE Transactions onWireless Communications 2018; 17(1): 352-360. doi: 10.1109/TWC.2017.2766620

[19] Hamamreh, JM, Hajar, A, Abewa, M. Orthogonal frequency division multiplexing with subcarrier power modulation for doubling the spectral efficiency of 6G and beyond networks. Trans Emerging Tel Tech. 2020; 31:e3921. https://doi.org/10.1002/ett.3921

[20] A. Jaradat, J. Hamamreh, and H. Arslan, "Modulation options for OFDM-based waveforms: Classification, comparison,and future directions,"IEEEAccess, vol. 7, pp. 17 263–17 278, 2019

[21] Goldsmith, A. (2005). Wireless Communications. Cambridge: Cam-bridge University Press. doi:10.1017/CBO97805118412

[22] Soury, H., Yilmaz, F., & Alouini, M.-S. (2013). Error Rates of M-PAM and M-QAM in Generalized Fading and Generalized Gaussian Noise Environments. IEEE Communications Letters, 17(10), 1932–1935. doi:10.1109/lcomm.2013.081913.131409

[23] H. Soury, F. Yilmaz, and M.-S. Alouini, "Average bit error probability of binary coherent signaling over generalized fading channels subject to additive generalized Gaussian noise," IEEE Commun. Lett., vol. 16, no. 6, pp. 785–788, June 2012.

[24] Sahin, Mehmet Mert Arslan, Huseyin. (2020). Waveform-Domain NOMA: The Future of Multiple Access.

[25] L. Dai, B. Wang, Z. Ding, Z. Wang, S. Chen and L. Hanzo, ”A Surveyof Non-Orthogonal Multiple Access for 5G,” in IEEE CommunicationsSurveys Tutorials, vol. 20, no. 3, pp. 2294-2323, thirdquarter 2018, doi:10.1109/COMST.2018.2835558.

[26] ——, “Study on Non-Orthogonal Multiple Access (NOMA) for NR,” 3rd Generation Partnership Project (3GPP), Technical Report (TR) 38.812, 12 2018, version 13.0.0.

[27] Clerckx, Bruno & Mao, Yijie & Schober, Robert & Jorswieck, Eduard & Love, David & Yuan, Jinhong & Hanzo, L. & Li, Geoffrey & Larsson, Erik & Caire, Giuseppe. (2021). Is NOMA Efficient in Multi-Antenna Networks? A Critical Look at Next Generation Multiple Access Techniques.

[28] Furqan, Haji M., Jehad Hamamreh, and Huseyin Arslan. ”Physical LayerSecurity for NOMA: Requirements, Merits, Challenges, and Recommendations.” arXiv preprint arXiv:1905.05064 (2019).

[29] Hamamreh, J. M., Abewa, M., & Lemayian, J. P. (2020). New Non-Orthogonal Transmission Schemes for Achieving Highly Efficient, Reliable, and Secure Multi-User Communications. RS Open Journal on Innovative Communication Technologies, 1(2). https://doi.org/10.46470/03d8ffbd.324cc0fb

[30] M. K. Simon and M.-S. Alouini, Fading Channel Characterization and Modeling. Hoboken, NJ, USA: Wiley, 2002, pp. 15–30.

[31] I.S.Gradshteyn and I.M.Ryzhik,Table of Integrals,Series and Products, 7th ed. San Diego, CA, USA: Academic, 2007.

[32] J. M. Hamamreh, E. Basar and H. Arslan, ”OFDM-Subcarrier Index Selection for Enhancing Security and Reliability of 5G URLLC Services,” in IEEE Access, vol. 5, pp. 25863-25875, 2017, doi: 10.1109/ACCESS.2017.2768558.

[33] Hajar, A., & Hamamreh, J. M. (2020). The Generalization of Orthogonal Frequency Division Multiplexing With Subcarrier Power Modulation to Quadrature Signal Constellations. RS Open Journal on Innovative Communication Technologies, 1(1). https://doi.org/10.21428/03d8ffbd.4948e89e

Thesis related Publications & Patents

Published Journal Papers:

---

1. Abewa, M., & Hamamreh, J. M. (2021). NC-OFDM-SPM: A Two-Dimensional Non-Coherent Modulation Scheme for Achieving the Coherent Performance of OFDM along with Sending an Additional Data-stream. RS Open Journal on Innovative Communication Technologies, 2(3). https://doi.org/10.46470/03d8ffbd.a97a5236
2. Hamamreh, J. M., Abewa, M., & Lemayian, J. P. (2020). New Non-Orthogonal Transmission Schemes for Achieving Highly Efficient, Reliable, and Secure Multi-User Communications. RS Open Journal on Innovative Communication Technologies, 1(2). https://doi.org/10.46470/03d8ffbd.324cc0fb
3. Abewa, M., & Hamamreh, J. M. (2020). Non-coherent OFDM-Subcarrier Power Modulation for Low Complexity and High Throughput IoT Applications. RS Open Journal on Innovative Communication Technologies, 1(1). https://doi.org/10.46470/03d8ffbd.2a45a9a1
4. Hamamreh, Jehad & Hajar, Abdulwahab & Abewa, Mohamedou. (2020). Orthogonal frequency division multiplexing with subcarrier power modulation for doubling the spectral efficiency of 6G and beyond networks. Transactions on Emerging Telecommunications Technologies. 31. 10.1002/ett.3921.

Papers Under Review / In Progress:

---

1. Abewa, M., & Hamamreh, J. M. (2021). Multi-User Auxiliary Signal Superposition Transmission (MU-ASST) for Secure and Low-Complex Multiple Access Communications.
2. Abewa, M., & Hamamreh, Mohamedou, Multi-User Auxiliary Signal Superposition Transmission (MU-ASST) with OFDM Subcarrier Power Modulation (SPM) for Doubling the Spectral Efficiency per Area and per Device in Future Wireless Systems.

Patent Applications:

---

1. Hamamreh, J. & Abewa, M., Non-Coherent OFDM with Subcarrier Power Modulation (NC-OFDM-SPM)
2. Hamamreh, J. & Abewa, M., Multi-User Auxiliary Signal Superposition Transmission (MU-AS-ST)
3. Hamamreh, J. & Abewa, M., Doubling the Spectral Efficiency per Area and per Device for wireless systems (D-SEAD)